On the Precipitation in Aluminium-Zinc-Magnesium Alloys

AUTHOR(S):

MURAKAMI, Yotaro; KOMATSU, Shinya; NAGATA, Koji

CITATION:

MURAKAMI, Yotaro ...[et al]. On the Precipitation in Aluminium-Zinc-Magnesium Alloys. Memoirs of the Faculty of Engineering, Kyoto University 1967, 29(2): 161-196

ISSUE DATE:

1967-06-10

URL:

http://hdl.handle.net/2433/280689

On the Precipitation in Aluminium-Zinc-Magnesium Alloys

By

Yotaro MURAKAMI*, Shinya KOMATSU* and Koji NAGATA**

(Received December 28, 1966)

The precipitation characteristics in Al-5wt% Zn-2wt% Mg alloys with or without a trace addition of Ag, Cu or Cr have been studied as the function of solution temperature and time, quenching temperature and medium, and pre-aging between quenching and artificial aging mainly by electrical resistivity measurement and tensile test.

Imperfections such as sub-boundaries still remained after incomplete solution treatment, though it is particularly the case when added Cr, influence remarkably the following precipitation. Vacancy-solute clusters, which could be formed during or immediately after quenching, can act as precipitation nuclei of η' intermediate phase and, therefore, influence considerably the age-hardening at higher temperatures. Pre-aging and small additions of Ag have also many favorable effects on higher temperature aging.

I Introduction

The high strength potentialities of heat-treated aluminium alloys containing a predominance of zinc have been known, and susceptibility toward stress corrosion cracking, a serious limitation to materials of this type, has been minimized through adding chromium and manganese which are helpful in this respect. The Al-Zn-Mg-Cu alloys of 7000 series have come into prominence for applications requiring high strength. Recently, the medium strength alloy with decreasing contents of the principal hardeners, zinc and magnesium and without copper are put to practical use for welding construction material.[1,2,3,4,] The ternary equilibrium diagram of Al-Zn-Mg system has been reported by many investigators[5,6,7,8], and it has been reported that the solubilty limit at Al rich corner is larger than that of the Al-Cu-Mg system. This fact seems to be one of a cause of favorable quench sensitivity and age-hardening at room temperature. As the larger solubility limit also makes it possible to increase the amount of additional elements, there have been some studies about the effect of trace elements[9].

The precipitation sequence of this alloy has been clarified by X-ray technique[10], electron-microscopy[11,12,13,14] and hardness measurement, as

Spherical G.P. Zone—η' ($MgZn_2$) Transition Phase—η ($MgZn_2$) Equilibrium Phase.

* Department of Metallurgy

** formerly graduate studeut, is now Sumitomo Light Metal Industries Ltd., Nagoya.

In the case of a larger content of Mg than the stoichiometry of $MgZn_2$, a ternary compound T precipitates after η equilibrium phase. Marked age-hardening comes from zones and fine particles of transition phase.

The present investigation was undertaken in an attempt to obtain a more detailed picture of precipitation in Al-Zn-Mg alloys and in particular to examine the role of the lattice defects and effects of trace elements.

II Experimental Procedure

The ingots of $20\times20\times250$ mm were prepared from 99.99% purity Al, Zn, Mg, Ag, high purity mother alloys of Al-49.27wt% Cu and Al-7.36wt% Cr, under Ar atmosphere. After the soaking at 500°C for 12 hrs, the ingots were hot- rolled in the temperature range of 400–500°C to 10 mm and then cold drawn to 0.75 mm in diameter. The chemical compositions are shown in Table 1.

Table 1. Chemical composition of specimens (wt%).

Specimen No.	Zn	Mg	Ag	Cu	Cr	Si	Fe
1	5.24	2.08	—	0.002	—	0.007	0.003
2	5.13	1.99	0.39	0.001	—	0.006	0.003
3	5.31	2.22	0.84	0.001	—	0.006	0.003
4	5.29	1.98	—	0.24	—	0.006	0.003
5	5.19	2.16	—	0.71	—	0.006	0.003
6	5.37	2.14	—	0.001	0.10	0.006	0.002
7	4.82	1.94	—	0.001	0.17	0.006	0.002

The tensile test was carried out using Shimazu 1M-100 Instron type tensile tester, usually at room temperature with the gauge length of 50 mm and the strain rate of 6.67×10^{-4}/sec. The proof stress was calculated at 0.2% plastic strain in the stress-strain diagram.

Electrical resistivity was measured at the liquid nitrogen temeprature by usual potential method using Yokogawa P-7 type potentiometers. The pure aluminium wires of 0.3 mm in diameter were spot welded as current and potential leads. Specimens were fixed by four leads to a quartz holder and heat treated. To eliminate the effect of room temperature aging, specimens were dipped into liquid nitrogen bath within 15 sec after quenching.

Specimens were drop-quenched from a vertical electric furnace in which solution heat treatment was carried out, usually into -20°C brine. Either a water bath or silicon oil bath was used for the investigation of the effect of quenching rate. As for aging bath, poly-ethylene-glycol was employed below 130°C, and silicon oil above 150°C.

III Results and Discussions

It is generally assumed that a complete solid solution could be obtained by solution heat treatment. However, there is much qualitative evidence that impurity atoms such as Cr, Zr, Fe etc., hinder recrystallization. Then, even when the alloy containing such trace elements is solution-treated above the recrystallization temperature, there may remain many defects such as dislocations and sub-boundaries. These dislocation lines and sub-boundaries in the quenched alloy may be assumed to affect precipitation both by nucleation on the dislocation itself and by the absorption of excess vacancy from the matrix. Thus, the effect of trace elements on age-hardening should be investigated from the point of the precipitation from the incomplete solid solution matrix containing many defects.

III-I Recrystallization and dissolution during solution treatment.

Fig. 1 shows the set of isothermal annealing curves for as drawn specimens of no addition alloy. The specimens were annealed for upto 10^4 min at temperatures between 100°C and 450°C, and quenched into water, and then stored in liquid nitrogen bath till setting to the tensile tester to avoid the age-hardening at room temperature. As the present specimens were made through the repetition of hot

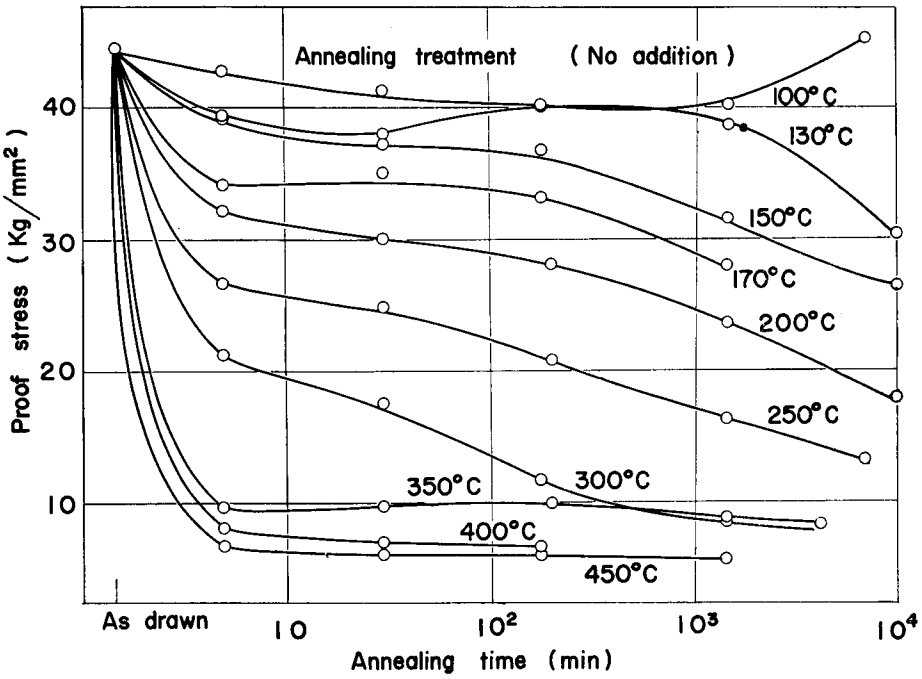

Fig. 1. Effect of isothermal annealing on 0.2% proof stress of the base alloy.

or cold deformation and annealing, the work hardening by clold deformation, the age-hardening at room temperature and the precipitation of large or small particles during cooling from hot rolling temperature may take place simultaneously. Therefore, the as-drawn specimen often exhibits the strength near the highest value obtained by the ordinary aging. As shown in Fig. 1, by annealing such specimens at 100–130°C, the softening occurs slowly at first, and the hardening takes place after 1 week which seems to be due to precipitation. In the temperature range of 150–300°C the softening takes place gradually, and rapidly above 350°C.

The isochronal annealing of 30 min was carried out in the temperature range of 300–525°C. Fig. 2 shows the change of 0.2% proof stress and electrical resistivity. Electrical resistivity was measured with the same specimen quenched repeatedly from each temperature. It is clear that the softening takes place in two stages, namely in the temperature range of 100–130°C (stage 1) and of 370–400°C (stage 2), but the resistivity increases in one stage. The temeprature at which the resistivity reaches nearly constant value coincides with that of 0.2% proof stress. Stress-strain curves in Fig. 3 show a serrated easy glide region near the starting point

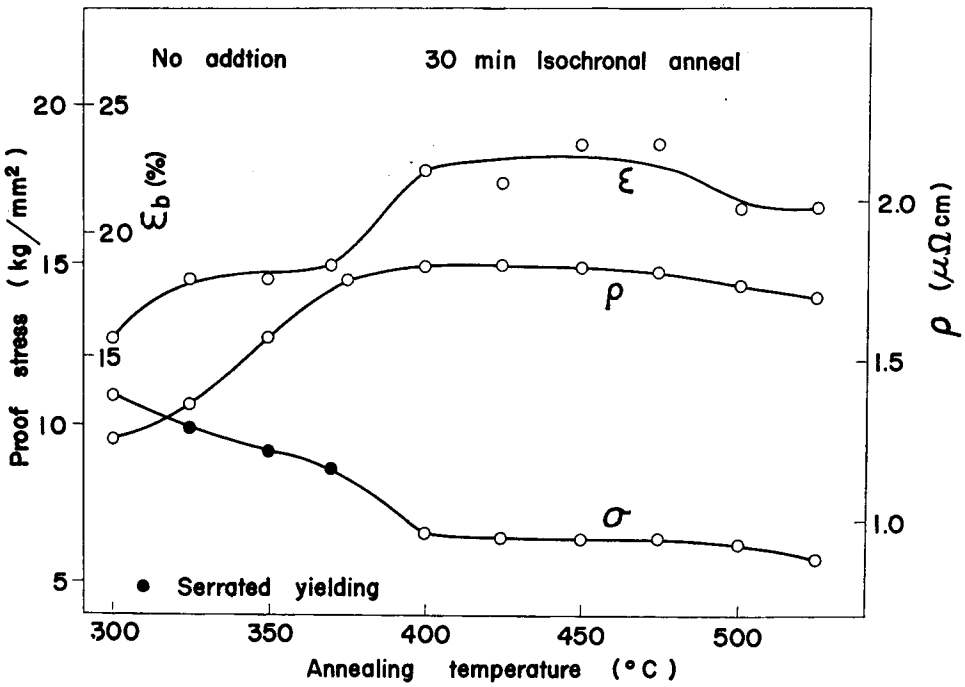

Fig. 2. Effect of isochronal annealing for 30 min on mechanical properties and electrical resistivity of the base alloy.

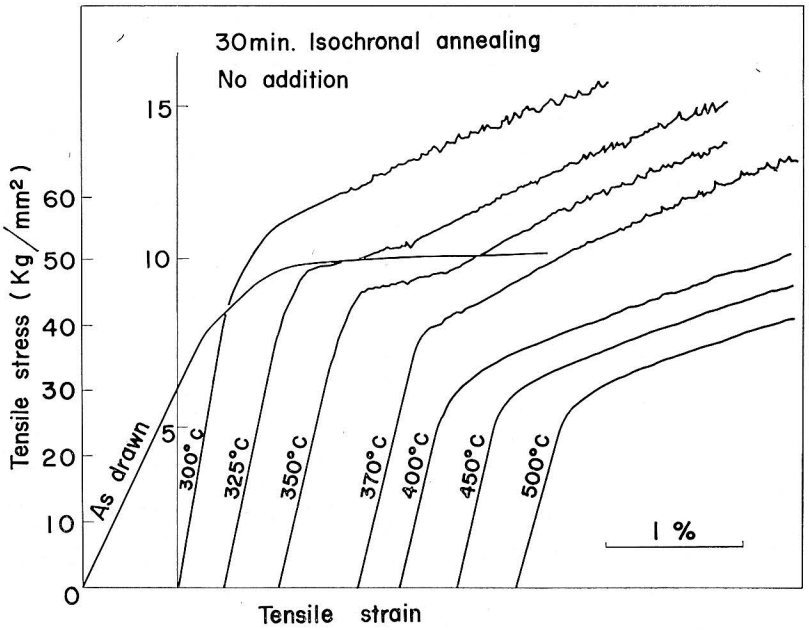

Fig. 3. Effect of isochronal annealing for 30 min on stress-strain curves of the base alloy.

of plastic deformation, which is well known in Al-Mg[15] or Al-Li[16] alloys, when annealed in a certain temperature range. This temperature range, which is determined to be 325–375°C in the case of the base alloy, corresponds to the range between completion of softening of stage 1 and start of stage 2.

Photo. 1 and Photo. 2 show the X-ray back reflection patterns. The specimen

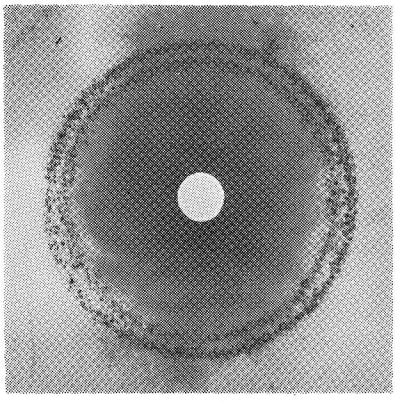

Photo. 1. X-ray diffraction pattern of Al-5 wt% Zn-2 wt% Mg alloy wire specimen annealed at 325°C for 30 min.

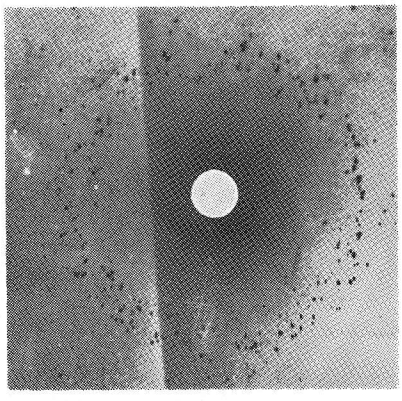

Photo. 2. Similar as Photo. 1, but annealed at 400°C for 30 min.

Table 2. Grain size in various heat treatment between 380°C and 550°C for Al-5 wt% Zn-2 wt% Mg alloy.

heat treaatment	380°C 2hr	450°C 2hr	550°C 2hr
grain size (μ)	50	300	650

annealed at 325°C for 30 min shows a nearly perfect ring, though at 400°C a marked grain growth is observed. Table 2 shows grain sizes of base specimen in some heat treatments.

From these results, the aspect of the structural change during solution treatment under the present condition of the specimens is thought to be as follows. The structure of cold drawn specimen would be a partially recovered one. Precipitates in matrix are small, but on grain boundaries they can grow to fairly large size and may be more stable than those in matrix. The small precipitates in matrix redissolve into solution at first and then tangled dislocations are re-distributed to make sub-boundaries. The serrated easy glide should take place in this stage. The disappearance of sub-boundaries and dissolution of large precipitates may occur at the temperature range between first and second stage of softening. When the solution treatment reaches this stage, the electrical resistivity will attain the saturated value.

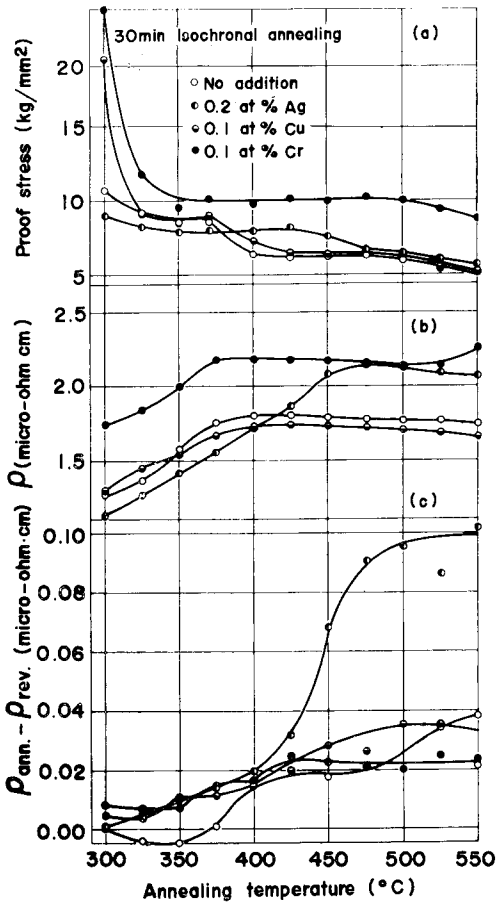

Fig. 4. Effect of isochronal annealing for 30 min on 0.2% proof stress and electrical resistivity of the alloys.
(a) change in 0.2% proof stress.
(b) change in electrical resistivity.
(c) difference in electrical resistivity between as-quenched state and aged state at 200°C for 1 min.

Effect of addition of trace elements on solution treatments.

The isochronal annealing for 30 min of the specimen containing 0.1 at % Cu, Cr and Ag respectively

was carried out similarly as in the case of base specimens. Fig. 4 shows that the value of 0.2% proof stress decreases in two stages, similarly as that of the base alloy. The temperature at which the electrical resistivity ceases to increase, coincides with the final temperature of proof stress decrease. This coincidence is also found to occur in alloys added Cu or Ag. On the other hand, in the case of specimen added 0.1 at % Cr, these temperatures are more elevated than other specimens. The temperatures corresponding to the completion of each stage are given in Table 3, together with the temperatures at which serrated yieldings

Table 3. The change of 0.2% proof stress, shape of stress-strain curves and electrical resistivity by isochronal annealing for 30 min at temperatures between 300°C and 550°C.

	0.2% Proof stress		s.y. apparent	smooth s.s. curve	resistance saturation temperature
	1st stage completion	2nd stage completion			
base	370°C	400°C	325°C~350°C	400°C	400°C
0.1 at % Cu	370°C	425°C	350°C~370°C	400°C	400°C
0.1 at % Cr	500°C	~550°C	350°C~500°C	550°C	550°C
0.2 at % Ag	425°C	474°C	325C°~400°C	450°C	475°C

are observable and disappear in the stress-strain curves, and also the temperatures at which electrical resistivity attains to the saturated value. The change of the shape of stress-strain curves with annealing is shown in Fig. 5. In Fig. 4 (c), the difference of specific resistivity between as-quenched state from various annealing temperatures and after a reversion of 200°C for 1 min. The decrease can be inferred to come from the dissolution of G.P. zone formed during quenching and in the period (max. 15 sec at room temperature) from quenching to dipping in liquid nitrogen bath, or from the decrease of solute atoms from matrix owing to the precipitation by aging at 200°C. The higher the quenching temperature, the greater the decrease occurs. It is not clear to what extent these two causes contribute, but this result generally agrees with vacancy theory. The specimen added Ag shows the greatest value in all specimens. This fact will be discussed later in terms of effects of Ag on nucleation.

Specific resistivity of each specimens.

The contribution of solute atoms in aluminium to the specific resistivity is reported in some papers[17] as regards Ag, Cu, Mg and Zn but there is no data about Cr. Therefore, electrical resistivity is measured with alloys containing 0.1 and 0.3 at% Cr respectively. The measurements were made at liquid nitrogen temperature on specimens quenched into −20°C brine after annealing at 550°C for 5 hrs. The

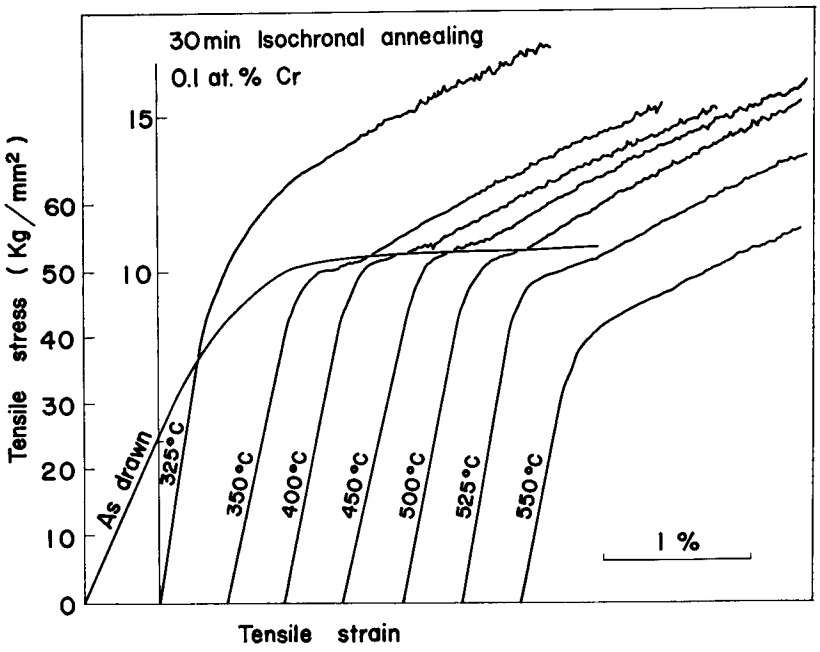
30min Isochronal annealing
0.1 at.% Cr
Tensile stress (Kg/mm²)
Tensile strain
As drawn
325°C
350°C
400°C
450°C
500°C
525°C
550°C
1 %

Fig. 5 (a)

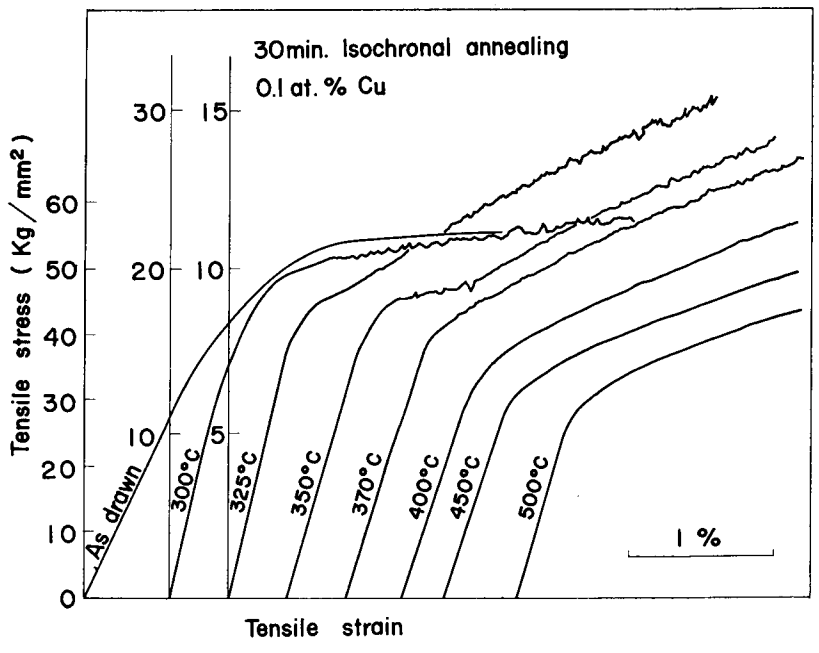
30min. Isochronal annealing
0.1 at.% Cu
Tensile stress (Kg/mm²)
Tensile strain
As drawn
300°C
325°C
350°C
370°C
400°C
450°C
500°C
1 %

Fig. 5 (b)

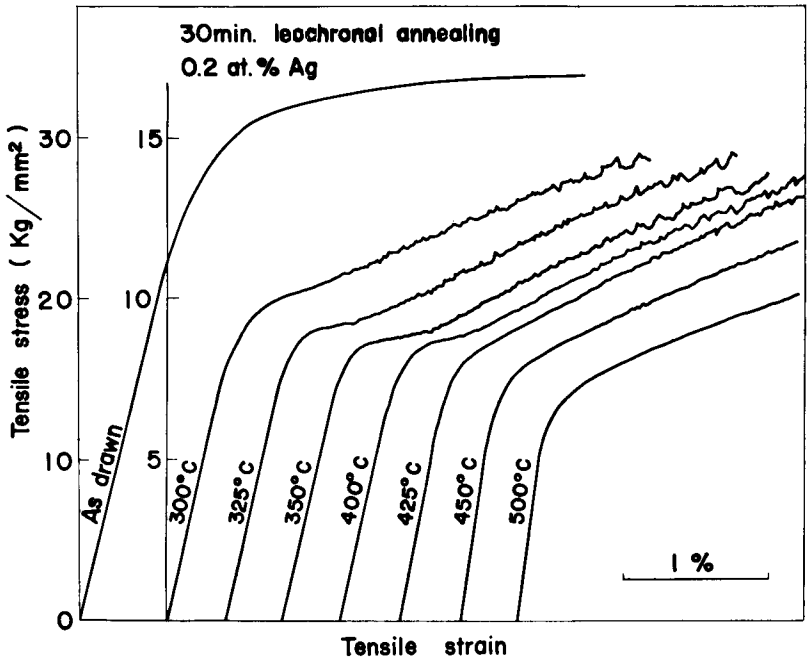

Fig. 5 (c)

Fig. 5. Effect of isochronal annealing for 30 min on stress-strain curves of
(a) specimen added 0.1 at% Cr.
(b) specimen added 0.1 at% Cu.
(c) specimen added 0.2 at% Ag.

contribution of Cr to resistivity calculated from the experimental value shown in Fig. 6 was confirmed to be 6.6 micro-ohm·cm/at%. Table 4. gives the contribution of each solute atom to resistivity in the concentration range between 0.1 and 0.5at%. The specific resistivity of each specimen is calculated from these values and chemical compositions shown in Table 1. The calculated and experimental values and the difference between base and other added alloys are shown in Table 5. The calculated values are always larger than experimental ones. This would be explained by the fact that the contribution per at% solute atoms may decrease with increasing solute concentration, and these values are obtained from the alloys in concentration range of 0.1–0.5 at%. In the case of the specimen with 0.1 at% Cr, the experimental value is by about 0.4 micro-ohm·cm higher than that of base specimen. This means that at least 60% of added Cr atoms are in solution and the remainder of Cr atoms precipitates as small particles which have a marked effect on the retarding of recrystallization.

In the previous chapter, it has become clear that the ideallized solid solution can not always be realized and many imperfections such as sub-boundaries still

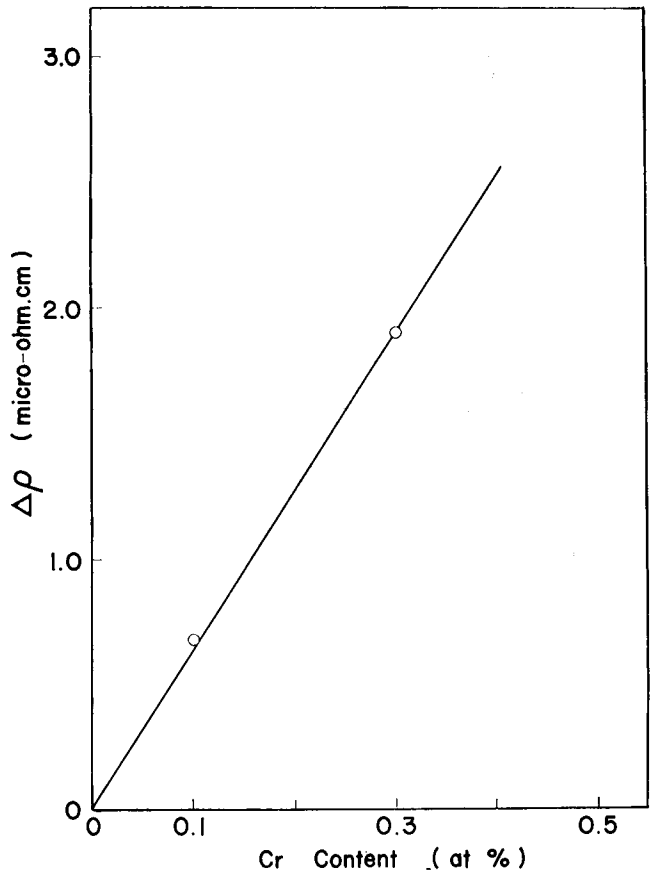

Fig. 6. Contribution of solute Cr on the electrical resistivity of Al (measured at 77°K).

Table 4. Contribution of solute elements on electrical resistivity of Al (measured at 77°K).

Zn	Mg	Cu	Cr	Ag
0.25	0.54	0.8	6.6	1.16

($\mu\Omega$ cm/at %)

Table 5. The comparison of the calculated and the observed value of electrical resistivity in as-quenched state and the difference between base alloy and alloys added 0.1 at % Cu, 0.1 at % Cr and 0.2 at % Ag, respectively.

Specimen	ρ cal	ρ abs	$\Delta\rho$ cal	$\Delta\rho$ obs
base	2.05	1.80	—	—
0.1 at % Cu	1.94	1.74	+0.11	+0.06
0.1 at % Cr	2.72	2.27(2.15)	−0.67	−0.35～−0.47
0.2 at % Ag	2.46	2.14	−0.40	−0.34

remain, being dependent upon the temperature and time of a solution heat treatment. The grain boundary and sub-boundary will act as vacancy sinks during quenching and hence vacancy concentration is changed. A more detailed study of this effect has been done by solution treatments at various temperatures, followed by quenching into —20°C brine and aging at 100°C and 170°C. Fig. 7 shows the effect of a change in solution temperatures on 0.2% proof stress. When aged at 100°C, no difference is shown on the shape of isothermal aging curves at the solution temperatures above 400°C, but the rate of hardening diminishes a little when solution-treated at 350°C. Fig. 7 illustrates marked effects when the aging temperature is raised to 170°C. The peak value of 0.2% proof stress decreases with decreasing solution temperature. Especially when quenched from 350°C, there shows scarcely any age-hardening. In the case of quenching from 400°C after pre-annealing at 500°C for 30 min a higher peak value than normal quenching from

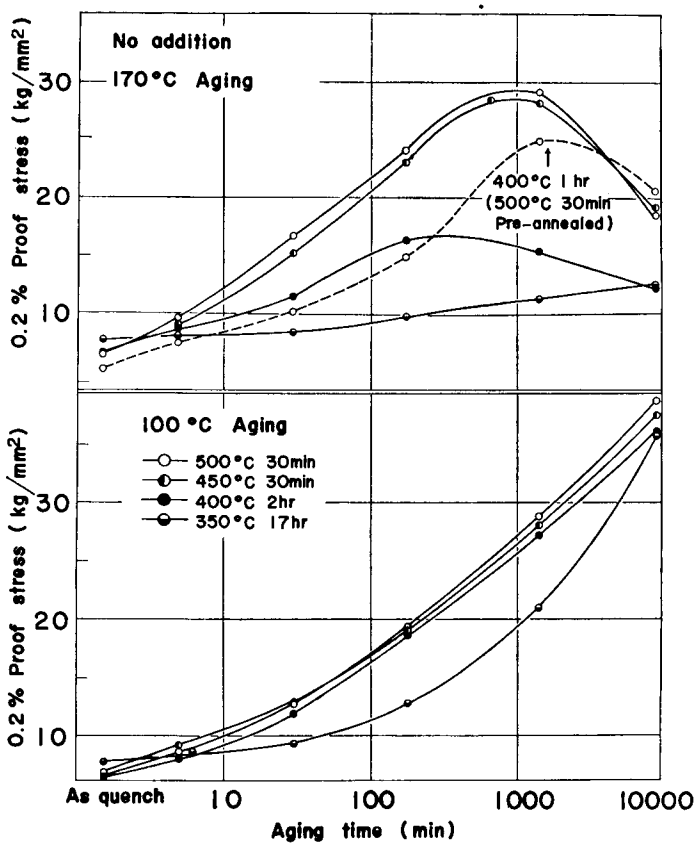

Fig. 7. Effect of solution treatment on 0.2% proof stress of the base alloy in aging at 100°C and 170°C.

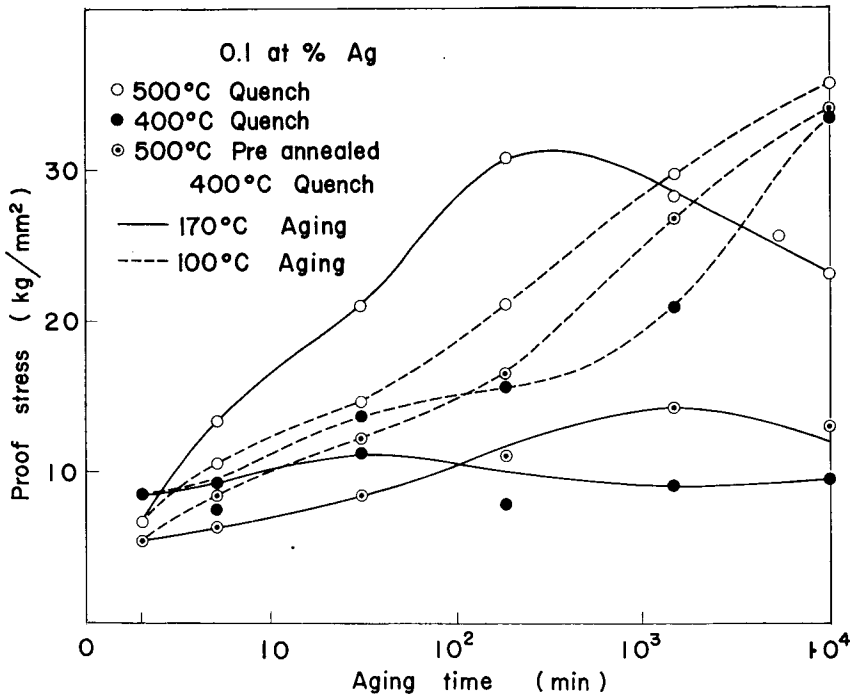
0.1 at % Ag
○ 500°C Quench
● 400°C Quench
◉ 500°C Pre annealed
400°C Quench
170°C Aging
100°C Aging
Proof stress (kg/mm²)
30
20
10
0
10
10²
10³
10⁴
Aging time (min)

Fig. 8 (a)

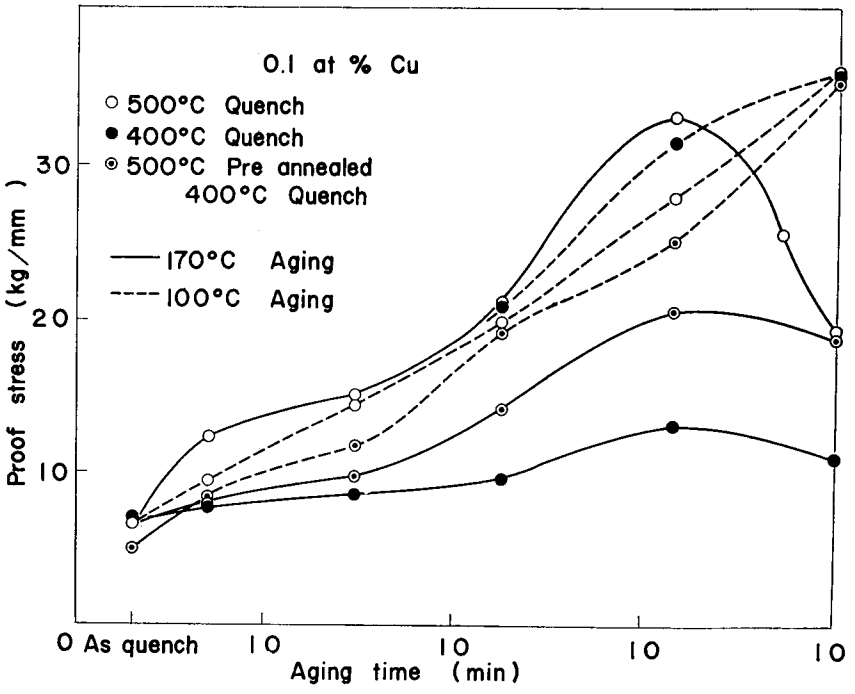
0.1 at % Cu
○ 500°C Quench
● 400°C Quench
◉ 500°C Pre annealed
400°C Quench
170°C Aging
100°C Aging
Proof stress (kg/mm)
30
20
10
0 As quench
10
10
10
10
Aging time (min)

Fig. 8 (b)

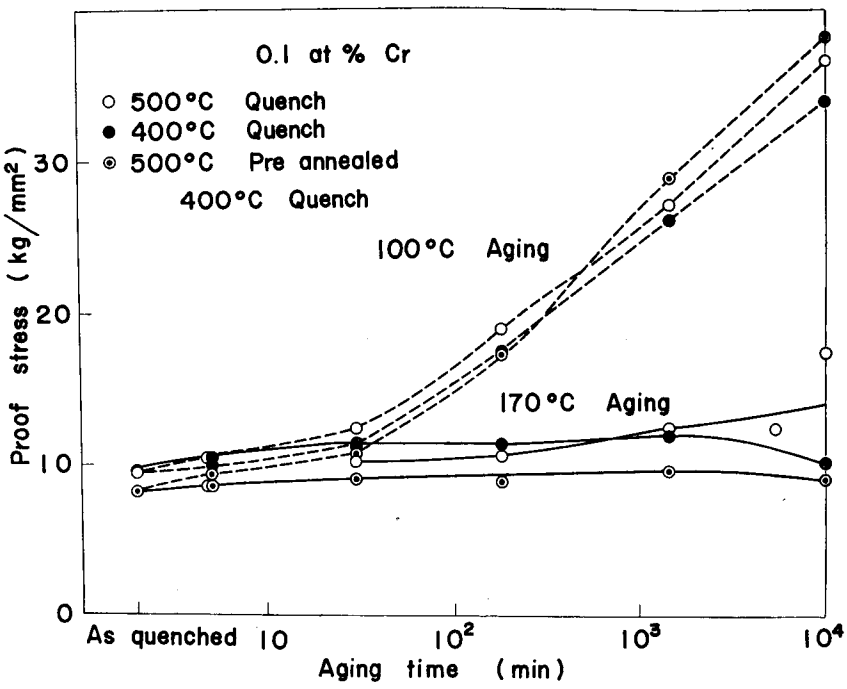

Fig. 8 (c)

Fig. 8. Effect of solution treatment on 0.2% proof stress in aging at 100°C and 170°C.
(a) specimen added 0.1 at% Ag.
(b) specimen added 0.1 at% Cu.
(c) specimen added 0.1 at% Cr.

400°C is seen. Then, it is concluded that the pre-annealing at 500°C regains the ability of age-hardening by obtaining the complete recrystallized state. There is no difference in aging curves between the specimens quenched from 450°C and 500°C. In Fig. 8 a), b) and c), the results of an experiment similar to the above are shown with alloys containing Ag, Cu and Cr. When aged at 100°C, the specimens containing Cu and Cr show no difference from the base specimen, but an addition of Ag causes a retardation of age-hardening when quenched from 400°C. In the case of 170°C, when solution-treated at 400°C, a lower hardening value is obtained in every specimen. This may be explained by the existence of retained sub-boundaries which act as vacancy sinks and nucleation sites of the intermediate phase. The solution treatment at 500°C causes a marked hardening in specimens containing Cu and Ag, but the specimen containing Cr, because of hindrance of the recrystallization[66], shows the poor age-hardening characteristics. When quenched from 400°C after pre-annealing at 500°C for 30 min, the similar effect as base specimen is given for the specimen containing Cu, but in the case of the specimen

containing Ag, it seems that the coarsening of precipitates takes place which results in the poor age-hardening characteristics. Now it is a problem whether the added elements completely dissolved or not. Considering the above results, we will be able to conclude that the solubility of Ag is smaller than that of Cu. When the solution treatment temperature is lowered to 400°C, the solubility limit of added Ag atoms is attained, then the precipitation of small particles occurs, which act as preferential nucleation sites for the intermediate phase.

III-II Isothermal aging of Al-Zn-Mg alloys.

In the present experiment, the maximum precipitation hardening occurs with the fine partial coherent η' metastable precipitates. Further aging causes the precipitation of block- or lath-shaped equilibrium phase. When the Mg content is larger than the stoichiometric composition of $MgZn_2$, the ternary compound $T((AlZn)_{49}Mg_{32})$ precipitates after η phase. The equilibrium phase η and T are non-coherent with matrix and precipitate as coarse particles. The strength of alloys is decreased on occurence of precipitation of these equilibrium phases. Species of these phases appearing in each stages of aging are affected by various factors such as aging temperature, ratio of Zn and Mg, addition of trace elements and quenching methods etc..

Thomas and Nutting[12], in an electron micrographic study of Al-3.2wt% Zn-2.5wt% Mg alloy, observed zones of 50 Å and $10^{15}/cm^3$ of density by aging at 160°C. The maximum strength was given by aging for 5 hrs at this temperature and in this stage η' particles (50 Å in diameter and $2\times10^{16}/cm^3$ of density) and a small number of zones are observed. Nicholson et al.[13,14] have reported similar results as above and suggested that the strengthening in this case may be mainly due to the dispersion hardening mechanism proposed by Orowan and Hirsh[18,19]. Polmear[9] concluded from the study of hardening of Al-4wt% Zn-3wt% Mg alloy that G.P. zone is stable below 135°C and this range is elevated to 155°C by the addition of 0.1at% Ag. Above this range, the zone is unstable and η' precipitates. In this section, aging properties are investigated by tensile test and electrical resistivity measurements.

Resistometric study of as-quenched state and aged state.

A much knowledge of the mechanism of clustering and formation of zone or transition phase has recently been obtained by resistivity measurements[23,24,63]. At first, the specific electrical resistivity was measured to study the as-quenched state. The measurements were made at liquid nitrogen temperature. The specimens were quenched from the temperatures in the range from 400°C to 500°C

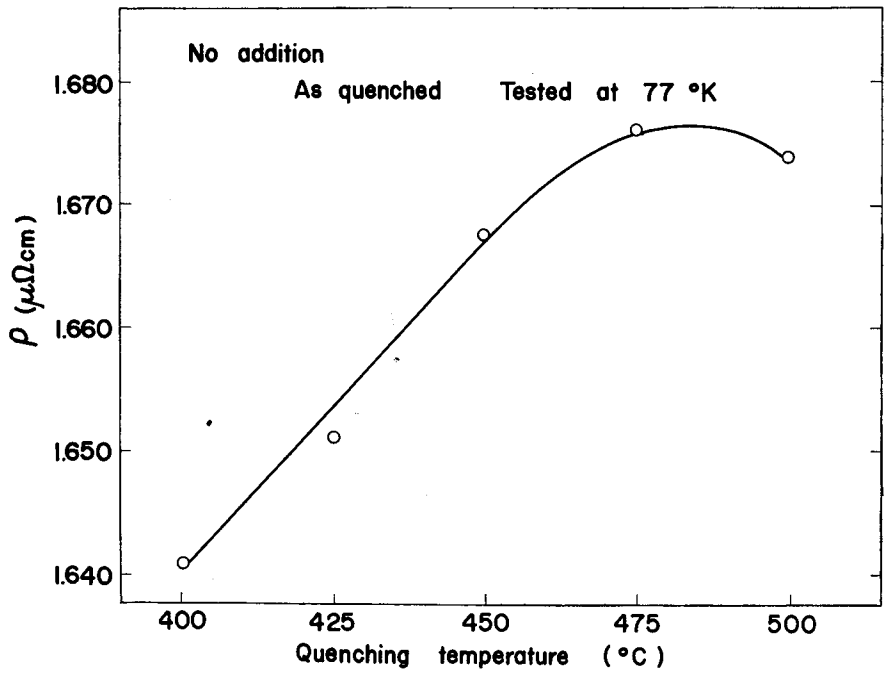

Fig. 9. Effect of quenching temperature on the as-quenched value of electrical resistivity of the base alloy.

after solution treatment at 500°C for 1 hr. Fig. 9 shows the effect of quenching temperatures on the as-quenched value of specific resistivity. The difference between the values of 400°C and 500°C seems to be considerably larger than the estimated value from the vacancy concentration. This means that an explanation of the difference must involve consideration of the effect of vacancy-solute clustering during quenching. In the first place, isothermal aging was carried out to study a low temperature aging. Specimens were quenched to —20°C brine after solution treatment at 450°C for 2 hrs and aged immediately at —20°C and 70°C. Reaging was carried out at 70°C on the specimens which were aged at 70°C for 3 days and then reversed at 200°C for 1 min. The isothermal curves obtained are shown in Fig. 10, where the variation in resistivity are expressed as a function of log time. Fig. 11 shows the initial part of the isothermal curves, where time is expressed linearly. ρ_0 for direct aging is the resistivity of the specimen in the as-quenched condition, and that for reaging is the one after reversion. The effect of the aging condition on resistivity is considerably large. It is well to distinguish between the isothermal curve at 70°C obtained by direct aging and that recorded by reaging. The curve of direct aging at 70°C shows that there exist the

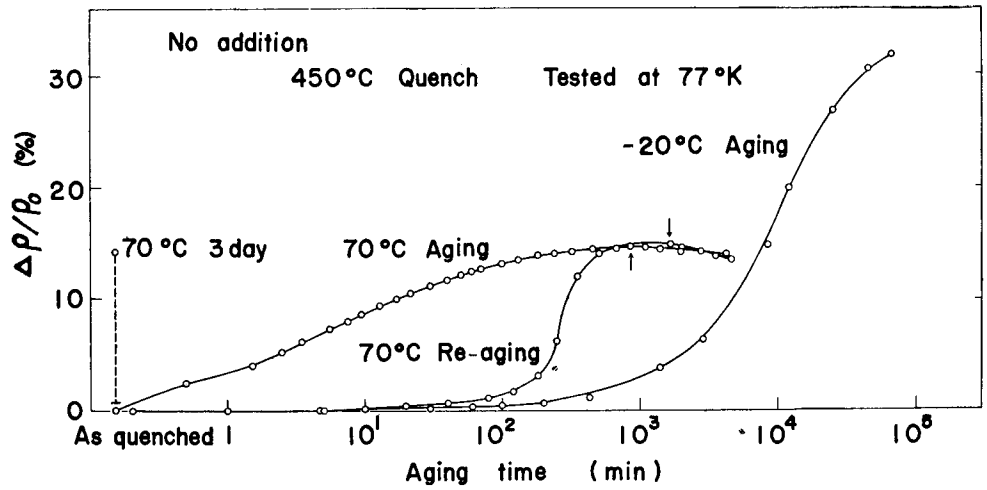

Fig. 10. Variation of the electrical resistivity with isothermal aging, plotted vs. logarithmic aging time.

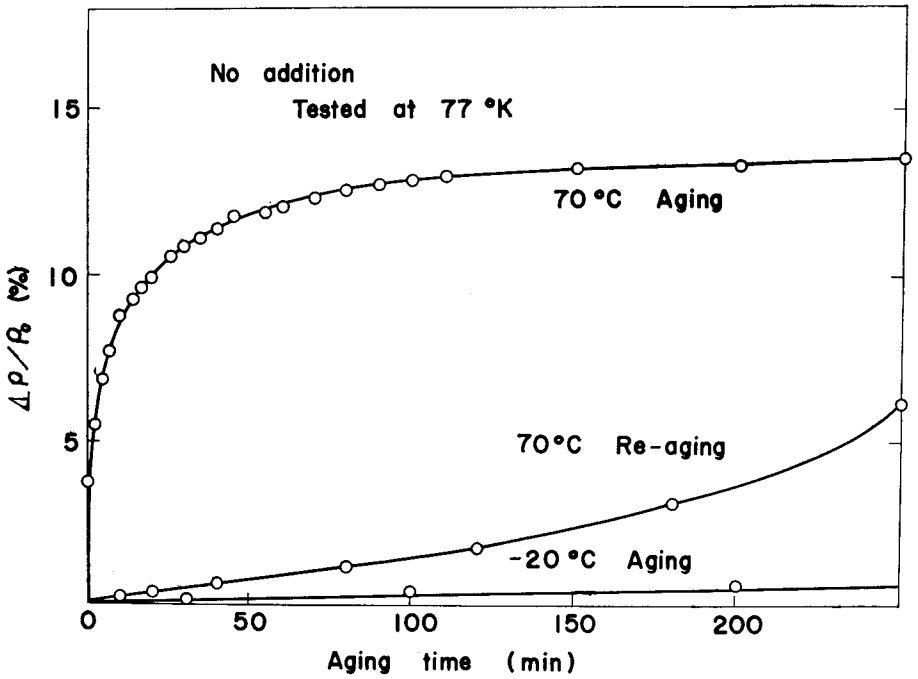

Fig. 11. Variation of the electrical resistivity with isothermal aging, plotted vs. natural aging time.

fast and slow reactions similar to Al-Cu alloy. This shows that the concentration of quenched-in vacancies and migration of diffusing entity act the great role in the rate of zone formation. In the case of aging at −20°C and reaging at 70°C, the

rate of increase in resistivity becomes very small, and particularly in the latter case there is no sign of any resistivity peak after 10^5 min.

Federighi and Thomas[29] assumed that the energy of binding between vacancies and G.P. zone is a very important factor to determine the aging behaviour. When a substantial energy of binding exists between vacancies and G.P. zones, vacancies will be trapped in G.P. zones. After the fast reaction a state of equilibrium between the vacancies arriving at the zones and those leaving will be established. Accordingly, from that moment the reaction will continue more slowly. To determine the critical aging temperature at which resistivity increase is observed, the isothermal aging was carried out at 100°C, 130°C and 150°C, respectively. The relation between aging time and variation in resistivity are shown in Fig. 12. Resistivity increases appreciably during aging at 100°C, but decreases in the case of aging at 150°C. When aged at 130°C, having reached a peak rapidly, there is a slow decrease in resistivity. The peak in resistivity may be interpreted as the results of overlapping of the increase by zone formation and the decrease by precipitation of transition phase. Therefore, the time needed to reach the peak is shortened by aging at a higher temperature. In the case of aging at 150°C, resistivity decrease may be explained from the fact that the time necessary to reach the

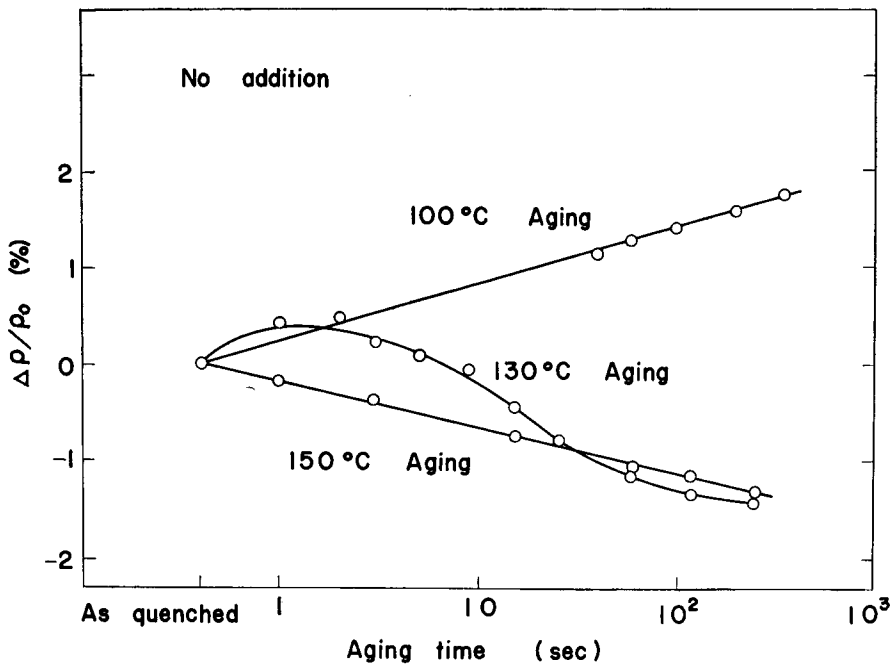

Fig. 12. Variation of the electrical resistivity with isothermal aging near the critical temperature of resistivity increase.

maximum resistivity is too short to be detected by the present method or that the decrease in resistivity by the formation of transition phase is larger than the increase by zone formation.

The change of proof stress by aging.

It may be supposed from the results of many studies about this alloy[9] that the zone hardening occurs below 100°C and the hardening above 130°C comes from the precipitation of transition phase. Some solute-vacancy clusters are formed in this alloy during quenching or immediately after quenching as mentioned above. The contribution of these clusters to the hardening was investigated. The same heat treatment as in the case of electrical resistivity measurements was carried out, namely quenching to −20°C brine from temperature range between 400°C and 500°C after pre-annealing at 535°C for 1 hr and aging at 70°C and 200°C. The effect of quenching temperature on 0.2% proof stress is shown in Fig. 13.

From the results of resistivity measurements, the size and number of clusters seems to depend considerably upon the quenching temperature, however, the 0.2% proof stress of the as-quenched specimens is not influenced by quenching

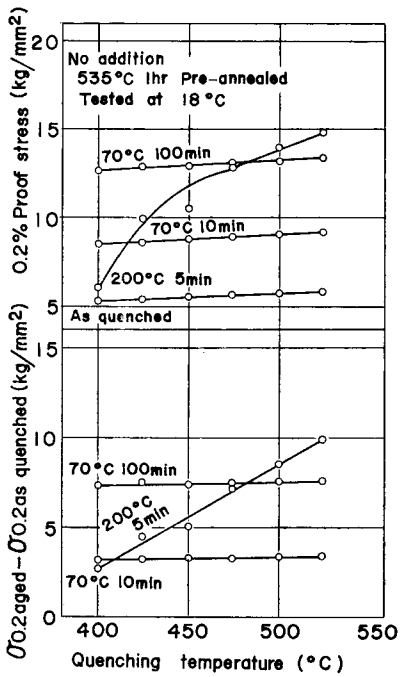

Fig. 13. Effect of quenching temperature on 0.2% proof stress in several aging treatments (upper part), and the increase of 0.2% proof stress from as-quenched state (lower part).

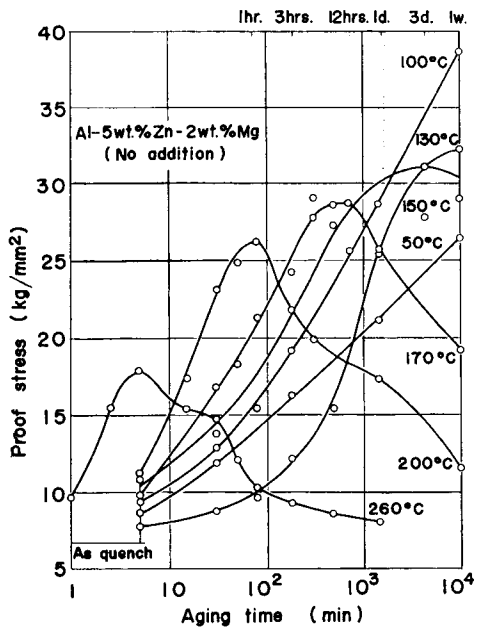

Fig. 14. Isothermal age-hardening curves of the base alloy.

temperature. This fact may be explained by the difference of the contribution of clusters to the resistivity and strength. The effect of clusters on strength is less marked than that on resistivity. The effect of quenching temperature on 70°C aging is also very small, but that on 200°C aging is very considerable. This result shows that cluseters formed during quenching influence the precipitation of transition phase rather than zone formation. This problem will be discussed later in terms of nucleation of transition phase.

The isothermal aging was carried out at several temeperatures in the range between 50°C and 260°C upto 1 week. The relations between 0.2% proof stress and aging time are shown in Fig. 14. A certain incubation period observed in the aging at the temperatures above 130°C is not appeared below 100°C. The maximum value and the aging time necessary to reach maximum decrease with increasing aging temperatures. These values are shown in Table 6. The relation be-

Table 6. Relation between the times to reach the maximum in 0.2% proof stress and its values at various aging temperatures.

Aging temperature	130°C	150°C	170°C	200°C	260°C
σ_{max} (kg/mm^2)	32	30	28	26	18
t_{max} (min)	$1\sim2\times10^4$	1.5×10^3	500	80	5

tween aging temperature and the time to reach maximum is plotted in Fig. 15. The apparent activation energy for the precipitation of transition phase is calculated as 1.10 eV from these plots.

The previously proposed mechanism of age-hardening may be devided into two groups according to the mode of interaction between dislocations and precipitates. One is the case of existing of long range interaction caused by stress field around precipitates. The G.P. zone is spherical in this alloy, therefore, only the short range interaction is to be considered. It is reported that the spherical G.P. zone is cut by dislocation, and the stress necessary to cut the G.P. zone depends only on the volume fraction of precipitates. Then, the strength should show monotonous increasing with aging when above condition is satisfied. The hardening part of isothermal aging curves will correspond to zone cutting. It is expected from theories about age-hardening that the volume fraction of precipitates will be almost constant after the strength maximum and the competition growth of particles takes place. This assumption agrees with the present results of resistivity measurements in 200°C aging, as shown in Fig. 16. Namely, the points at which the rate of resistivity decrease markedly lessened is in fairly good agreement with starting point of strength decrease, as shown by arrows in Fig. 16.

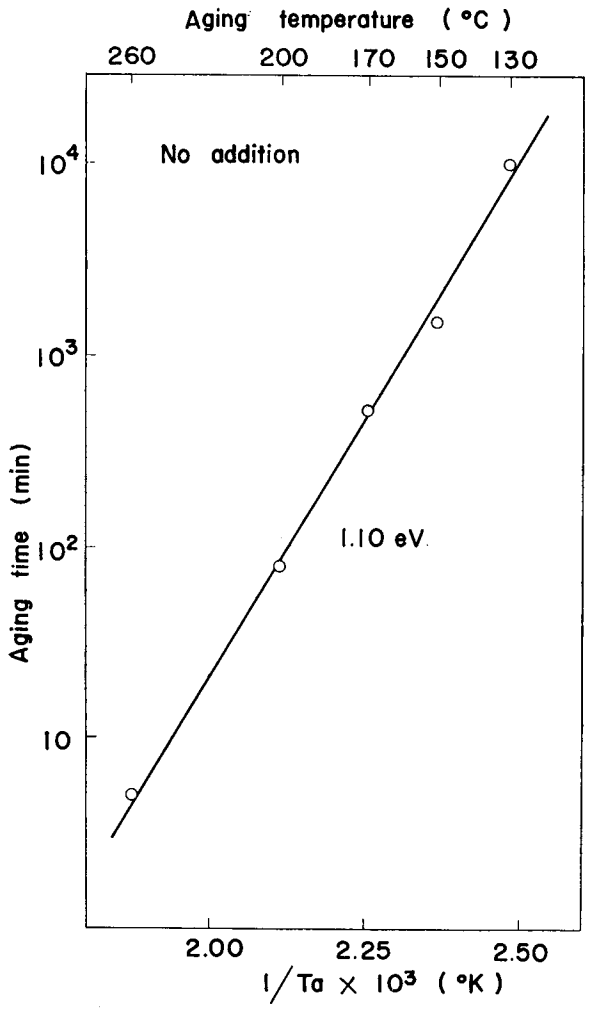

Fig. 15. Relation between the times to reach the maximum in 0.2% proof stress and the reciprocal of the absolute aging temperature.

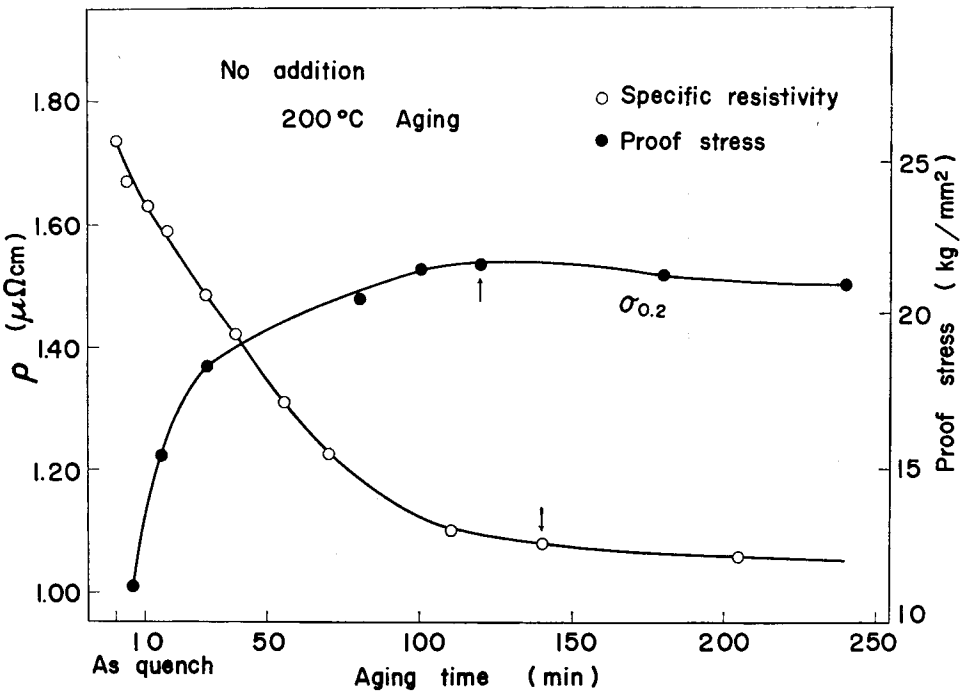

Fig. 16. Variation of the electrical resistivity and 0.2% proof stress by isothermal aging at 200°C for the base alloy, plotted against natural aging time.

The test temperature dependence of the strength.

The temperature dependence of the strength of age-hardening alloys are fairly important indices of the interaction between moving dislocations and particles of precipitates. In case of hardening by Orowan's mechanism or long range interaction, the dependence is very small as expected theoretically and confirmed experimentally. On the contrary, the test temperature dependence is very large in case of short range interaction such as zone cutting. Byrne[38] proposed two ways in cutting the zones of Al-Cu alloy, from extraordinary dependence on temperature. Thomas[40] suggested the existence of vacancies around zones and their interaction with dislocations. Dash et al.[37] supposed that the larger dependence in Al-Zn alloys than in Al-Ag alloys will come from generation of dislocations around the zones which is due to the difference in atomic size of Al and Zn or Ag.

To check whether dislocations cut the zones or not, the test temperature dependence is investigated in 70°C and 200°C aging. Specimens were annealed at 535°C for 1 hr and quenched from 450°C or 500°C into −20°C brine and immediately aged at 70°C for 1 or 100 min and at 200°C for 1, 10 and 100 min. The results obtained from tensile test at 77°K, 198°K and 288°K are shown in Figs. 17 and 18. The former shows the 0.2% proof stress vs. T and the latter the 0.2%

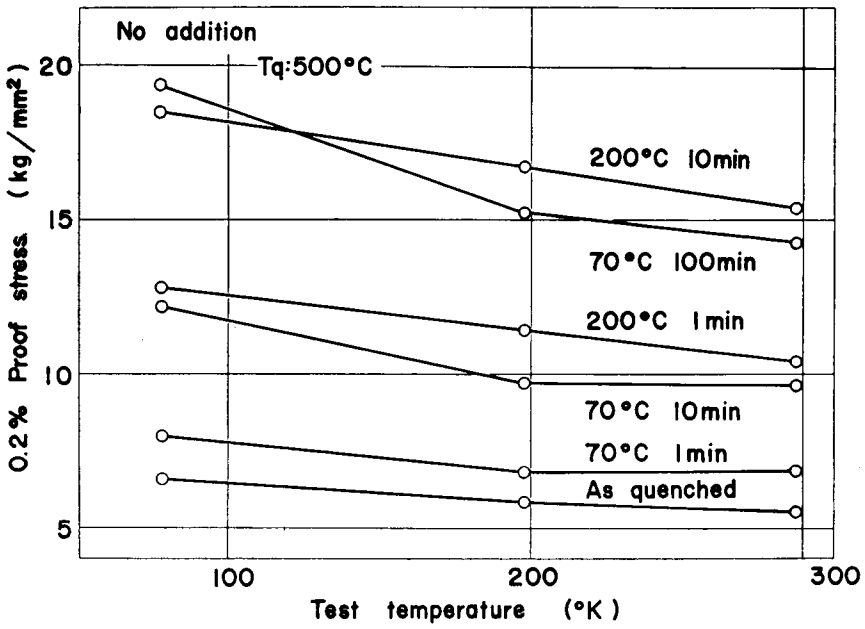

Fig. 17. Test temperature dependence of 0.2% proof stress of the base alloy after several aging treatments, plotted against normal test temperature.

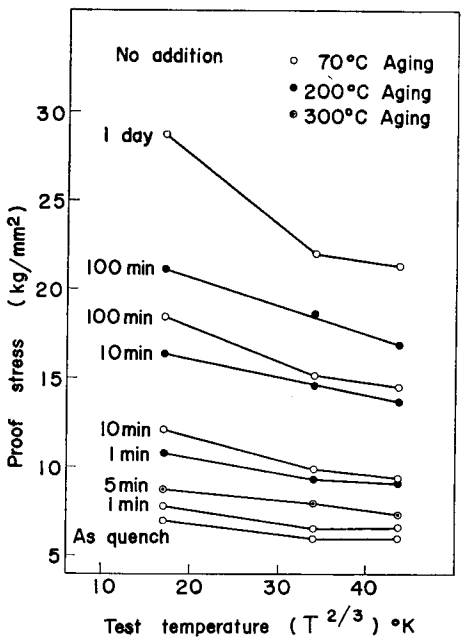

Fig. 18. Test temperature dependence of 0.2% proof stress of the base alloy after several aging treatments, plotted against $T^{2/3}$.

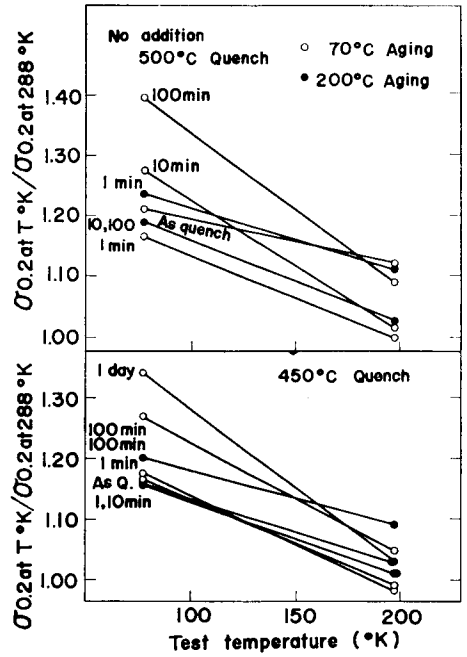

Fig. 19. Test temperature dependence of the ratio of 0.2% proof stress at 77°K and 198°K to that of at room temperature (288°K).

proof stress vs. $T^{2/3}$ plots. Two straight lines are shown in the case of as quenched or slightly aged specimen and with increasing aging time these two lines turn into a single straight line. The former relation is similar to the behaviour of Al-Cu containing G.P. zones. The latter is expected from the calculations done by Mott[35] and Seeger[36] according to the zone cutting theory and resembles the behaviour of Al-Cu alloy containing G.P. (II) zones or Al-Ag and Al-Zn alloys containing spherical zones. This discrepancy shows that the mechanism of deformation is not so simple because of the coexistence of zones and trnasition phases.

In Figs. 19 and 20 the results same as shown in Figs. 17 are rearranged in the ratio of strength at the two testing temperatures. In Fig. 19 the ratio of strength

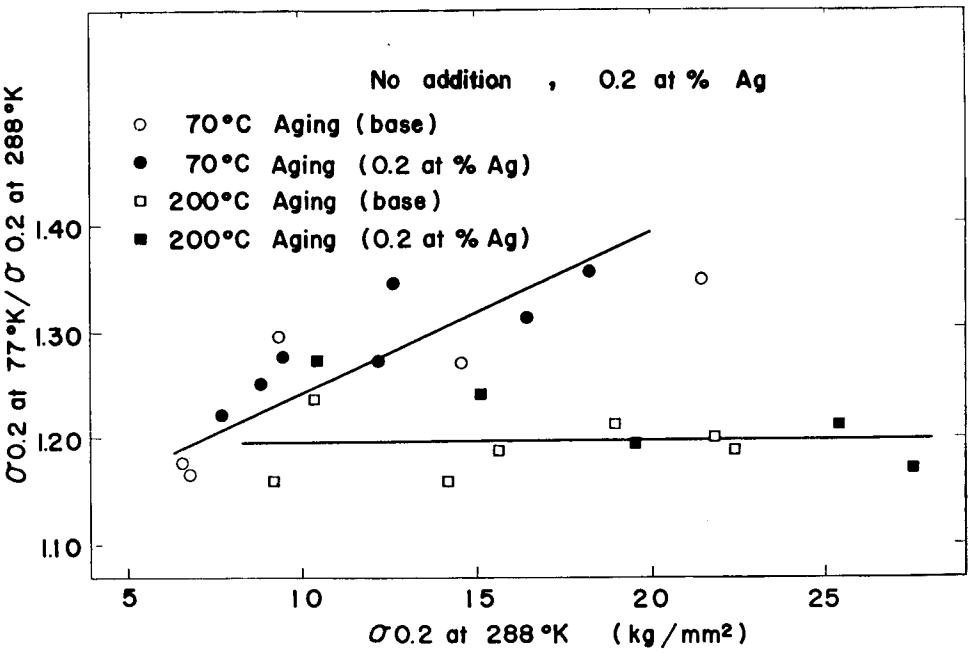

Fig. 20. Relation between the ratio of 0.2% proof stress at 77°K to that of at room temperature (288°K) and the 0.2% proof stress at room temperature.

($\sigma_{0.2}$ at 77°K/$\sigma_{0.2}$ at 288°K) was plotted to 0.2% proof stress at room temperature. The results of Dash et al.[37] and Price et al.[39] about Al alloys are put together with our results in Table 7. They assumed that the test temperature dependence increases with increasing ratio of strength at T°K to that at room temperature. The dependence is larger in 70°C aging than 200°C aging and this tendency increases with advance of aging. However, in 200°C aging, the ratio is constant with no relation to aging time. There is no model to explain the results shown in

Table 7. The ratio of 0.2% proof stress at 77°K and room temperature for Al, Al-Cu, Al-Ag, Al-Zn and Al-Zn-Mg alloys containing G.P. zones.

	$\sigma_{0.2}$ at 77°K/$\sigma_{0.2}$ at 288°K
pure Al (poly-crystal)	2.2～2.6
Al-6 wt % Ag [37].	1.13
Al-1.65 wt % Zn [37].	1.30
Al-5.28 wt % Zn [37].	1.24
Al-3.7 wt % Cu (G.P.II). [39]	1.23
Al-20 wt % Ag (zone) [39]	1.07
Al-15 wt % Zn (zone) [39].	1.13
Al-5 wt % Zn-2 wt % Mg (70°C 10 min)	1.29
(200°C 10 min)	1.16

Fig. 19, in which the more straight relations appear in specimens aged at high temperature than in specimens aged at low temperature. The results of Koda and Nemoto[64] shows that even noncoherent precipitates may be cut by dislocations when they are very small (e.g. smaller than 150Å in Al-Si alloy). The fact reported by Embury and Nicholson[14] suggests that the highest strength in isothermal aging is obtained when the particle size is close by above example.

III-III The nucleation of precipitates in an Al-Zn-Mg alloy.

The mechanism of nucleation of precipitates in higher temperature aging is a very important problem, because the size and distribution of the precipitates is one of the main factors of determining the strength of the age-hardening alloy. Some models of nucleation[27,41] have been proposed in which the main factor controlling nucleation is assumed to be the solute supersaturation. In recent years, it is clarified by transmission electron microscopic technique[30,42,43], that the degree of dispersion of precipitates is sensitive to quenching method, aging process[67] and the presence of trace elements. It was reported by Embury and Nicholson[14], that the factor to determine the degree of dispersion of precipitates is not only supersaturation of solute atom, but also the existence of excess vacancy, dislocation ring or other lattice defects. They have been used to develop a model of nucleation by vacancy-solute atom clusters.

In this experiment, the effects of quenching method and addition of Ag on the nucleation of precipitates investigated by tensile tests and electrical resistivity measurements. Moreover, the effect of zones formed by preceding low temperature aging on the aging behaviour at higher temperature is also studied.

The effect of quenching method.

In III-II, the formation of vacancy-solute clusters during quenching has been

confirmed by electrical resistivity measurements. Though the contribution to strength is very small in as-quenched state, the clusters can act as precipitation nuclei and influence the high temperature aging. Then, in this experiment, the aging behaviour was checked with various quenching conditions such as solution treatment temperature and quenching rate.

After the pre-annealing of 1 hr at 535°C, specimens were quenched into −20°C brine from several selected temperatures between 350°C and 525°C, and aged at 70°C or 200°C for 10 min. Fig. 21 shows the effect of quenching temperatures on the difference of electrical resistivity between as-quenched state and

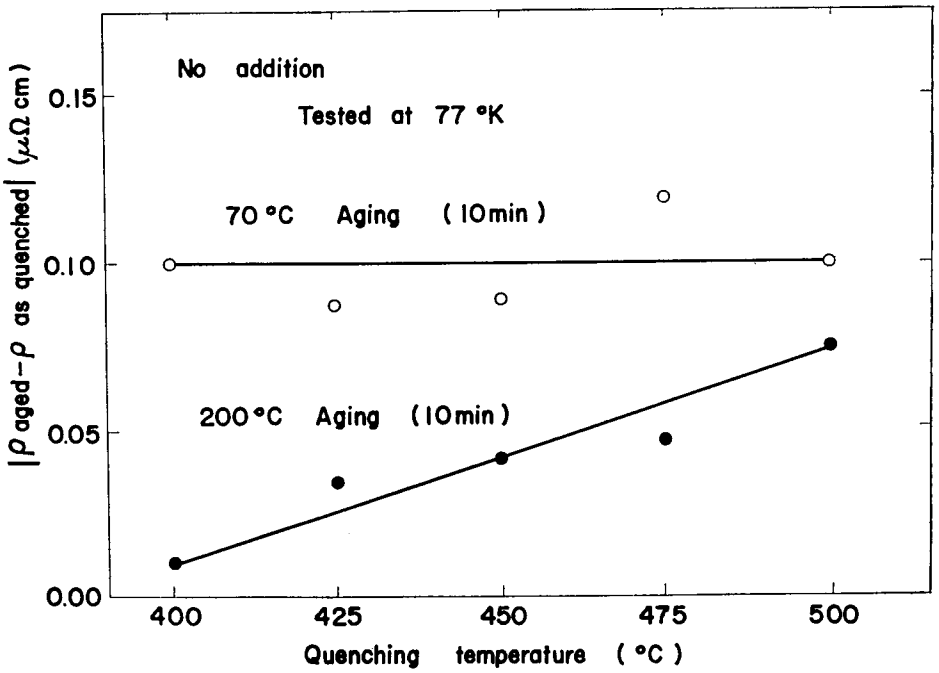

Fig. 21. Effect of quenching temperature on the absolute value of variation in electrical resistivity of base alloy after 10 min aging at 70°C and 200°C.

that of aged state. It is very interesting to note that the difference of electrical resistivity is not sensitive to the quenching temperature when aging is carried out at 70°C for 10 min, though higher quenching temperature has led to a great increase in resistivity difference in the case of aging at 200°C for 10 min. There is as large a difference as 0.06 micro-ohm·cm between 400°C and 500°C quenching. This resistivity difference is too large for the value which comes from a contribution of high concentration of excess vacancies in higher quenching temperature. It is natural that this is mainly due to high concentration of vacancy-solute clusters

formed during quenching. This leads to the suggestion that nucleation of η' precipitates is considerably dependent upon the number, size and distribution of the vacancy-solute clusters which is determined by the initial vacancy concentration, the quenching behaviour and other factors. This consideration is also proved by the fact that the strength varies quite similarly to the electrical resistivity, as shown in Fig. 22. Several aging treatments were carried out at 200°C after quenching from various solution treatment temperatures between 500°C and 350°C. The isothermal aging curves are shown in Fig. 23. The time needed to reach the peak of 0.2% proof stress becomes larger, the lower is the quenching

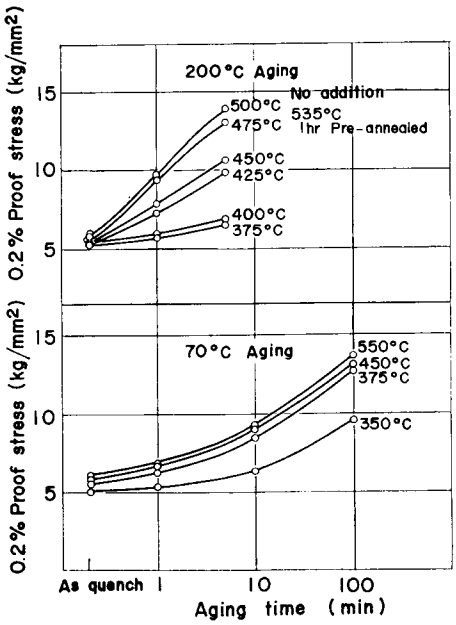

Fig. 22. Effect of quenching temperature on the age-hardening of base alloy at 200°C (upper part) and 70°C (lower part), after pre-annealing at 535°C for 1 hr.

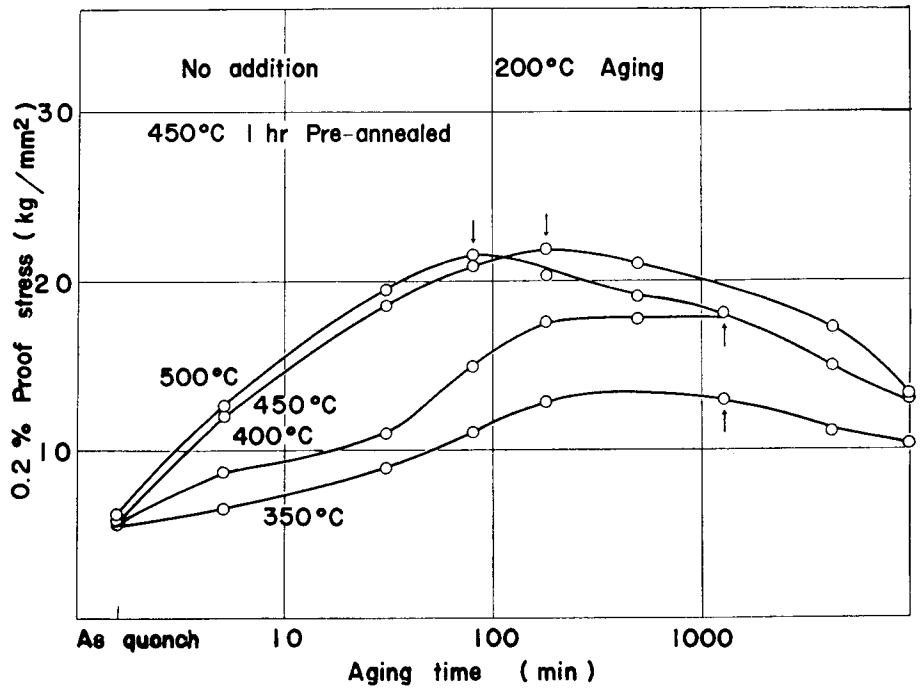

Fig. 23. Effect of quenching temperature on age-hardening of the base alloy at 200°C, after pre-annealing of 1 hr at 450°C.

temperature. There is only a little effect on low temperature aging, and it is to say that the relation between the concentration of vacancy-solute clusters and formation of G.P. zone is not as close as that in the case of precipitation of transition phase.

If the specimen is quenched from the same homogenizing temperature to various quenching medium such as brine, water, oil and air of various temperatures, the density of vacancy sinks being conserved, the concentration of quenched-in vacancy will depend on annihilation at sinks during quenching. In addition to the variation of total vacnacy concentration, the number, size and distribution of the clusters will vary with the quenching rate. From Fig. 24 which shows the effect of a change in quenching medium and quenching rate, it is clear that, as expected from quenching temperature effect, the effect is much larger in aging at 200°C than at 70°C.

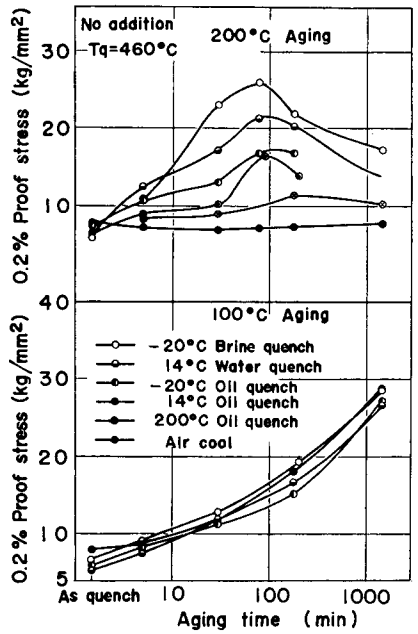

Fig. 24. Effect of the cooling rate on age-hardening of the base alloy at 200°C (upper part), and 100°C (lower part)

Taylor[43], Embury and Nicholson[14] reported from their electron microscopic observations that the width of precipitate free zone neighboring grain boundaries is remarkably dependent on quenching method and aging temperature. They[14] considered that the nucleation of precipitates is markedly influenced by the concentration and distribution of vacancies which existed in the supersaturated alloy after quenching. Nicholson et al.[14,65] have shown that the variation in microstructure with heat treatment can be adequately explained by a nucleation model involving vacancy-solute clusters.

The size distribution chart of the clusters is schematically shown in Fig. 25. The slower the specimen is quenched, the larger amount of vacancies are trapped and the larger the size of clusters becomes. When quenched from relatively low temperature, the equilibrium concentration of vacancies at homogenizing temperature and, therefore, the concentration of quenched-in vacancies is small. Thus the small number of large clusters is obtained by slow quenching or that

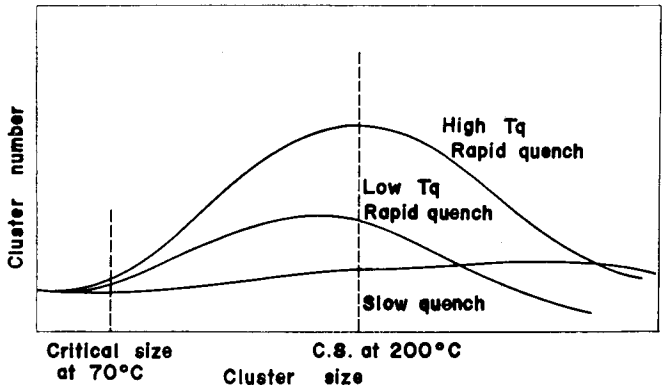

Fig. 25. Schematic representation of the size and the number of vacancy-solute clusters formed during or immediately after quenching.

from low temperature, and the large number of small clusters by rapid quenching. If the size distribution of clusters spreads over the critical size of nuclei, and aged at a higher temperature, clusters below the critical size will be dissolved with release of trapped vacancies and those above will continue to grow and act as nuclei. The effect of clusters on the resistivity or the strength of the alloys can be explained in the following way. The number of nuclei directly corresponds to the peak value of 0.2% proof stress and rate of age-hardening. On the contrary, clusters will show no effect on low temperature aging, because the hardening at low aging temperature is mainly due to G.P. zones which need no nucleation. The rate of age-hardening, as shown in Fig. 24, is scarcely dependent on a change in quenching medium, because the vacancy concentration enough for the formation of G.P. zone will be conserved by the existence of probably Mg atoms.

Effect of pre-aging at low temperature.

Recently much attention has been paid in the effect of a time interval between the quenching and artificial aging of aluminimu alloys. This delay can result in mechanical properties inferior or superior to those produced by immediate aging. Some reasons for the delay effects have been put forward, and some evidences have also been reported. The following experiments are carried out in order to clarify the influence of pre-aging and reversion on the artificial aging.

When the aging temperature is raised above the certain critical temperature after pre-aging at low temperature, partial reversion of G.P. zones and precipitation of a intermediate phase take place simultaneously. The higher the artificial aging temperature is, the larger will be the size at which a zone becomes stable,

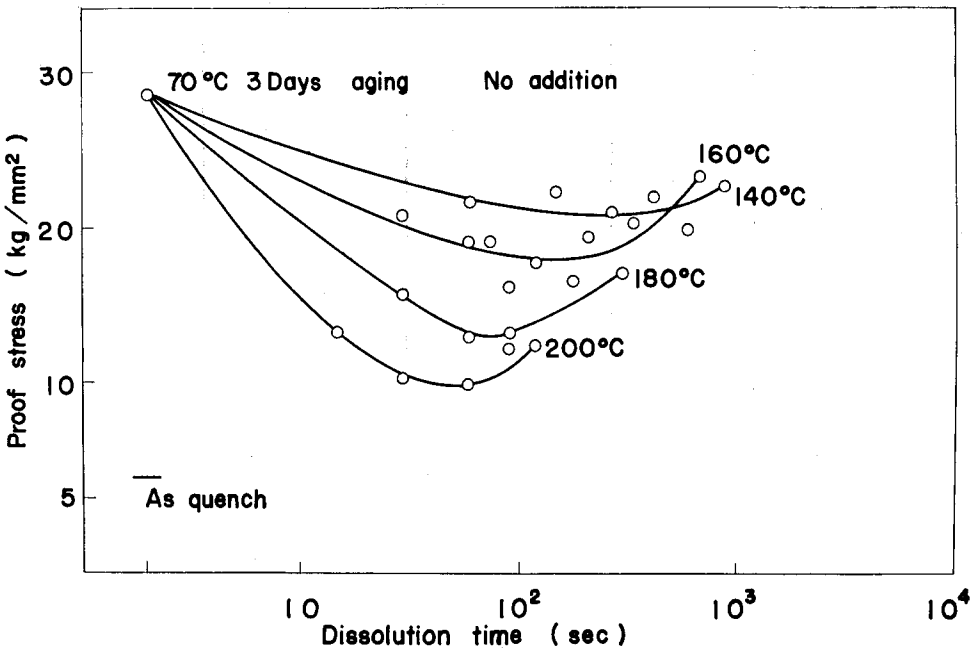

Fig. 26. Effect of dissolution treatment at various temperatures on 0.2% proof stress of the base alloy aged at 70°C for 30 min.

and some zones will continue to grow while others dissolve, and, therefore, changes take place in electrical and mechanical properties. Fig. 26 shows the reversion and precipitation curves for base alloys aged artificially at the temperatures in the range between 140 and 200°C for 5 to 10^3 sec, after aged at 70°C for 3 days. Fig. 27 shows the similar curves when aged at 200°C after pre-aged for 30 min and 3 days at 70°C and for 10 days at room temperature respectively. The decrease in 0.2% proof stress observed at first can be considered that G.P. zones smaller than the critical size are dissolved. The value of 0.2% proof stress reaches minimum and then increases again, corresponding with the precipitation of an intermediate phase. The decrease in 0.2% proof stress due to the dissolution of G.P. zones becomes larger and the time to the minimum becomes earlier, the higher the artificial aging temperature. The 0.2% proof stress of aging at 70°C for 30 min is decreased to as-quenched value by 5 sec when aged at 200°C, as shown in Fig. 27. This indicates that a complete reversion can occur when aged at 200°C after pre-aging at 70°C for 30 min for base alloys. On the contrary, when aged at the same temperature for 3 days no complete reversion takes place.

The effect of pre-aging treatment on 0.2% proof stress in the case of 200°C aging is shown in Fig. 28. Pre-aging for one week at 70°C is very effective to

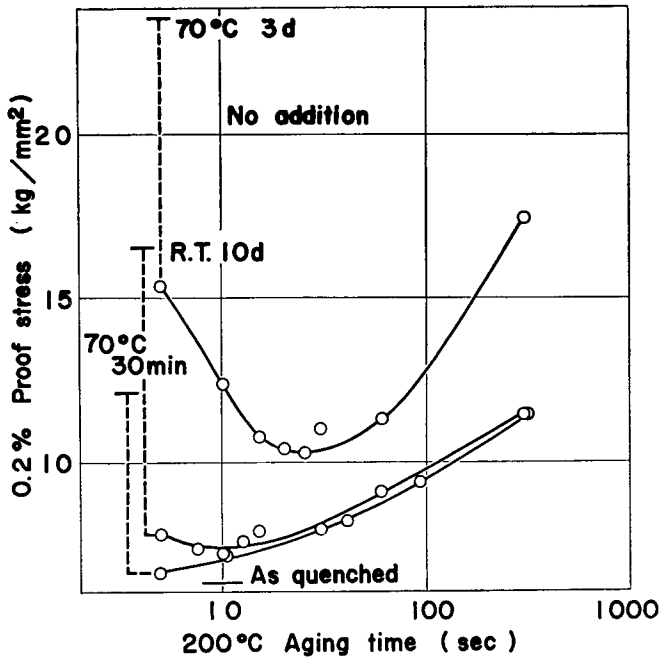

Fig. 27. Effect of dissolution treatment at 200°C on 0.2% proof stress of the base alloy after various aging treatments.

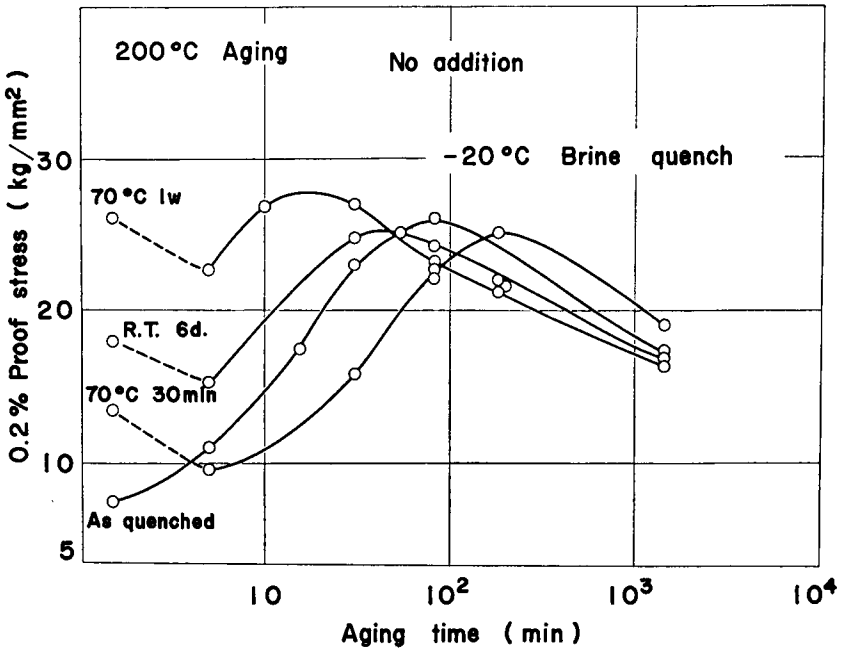

Fig. 28. Effect of various pre-aging treatments on the age-hardening of base alloy at 200°C.

increase the 0.2% proof stress of artificial aging at 200°C, though 30 min at the same temperature is not sufficient. The suitable pre-aging is very effective to increase the maximum strength and to decrease the time necessary to reach the maximum strength.

The curves in Fig. 29 show that the effect is to increase the 0.2% proof stress of the specimen quenched slowly, such as, into a oil bath of 14°C or air cooled, when artificially aged at 200°C. These results mentioned above indicate that pre-aging increases considerably the rate of hardening in the case of higher temperature aging. This must mean that the clustering process is sufficiently affected for finer precipitate distributions to generally occur.

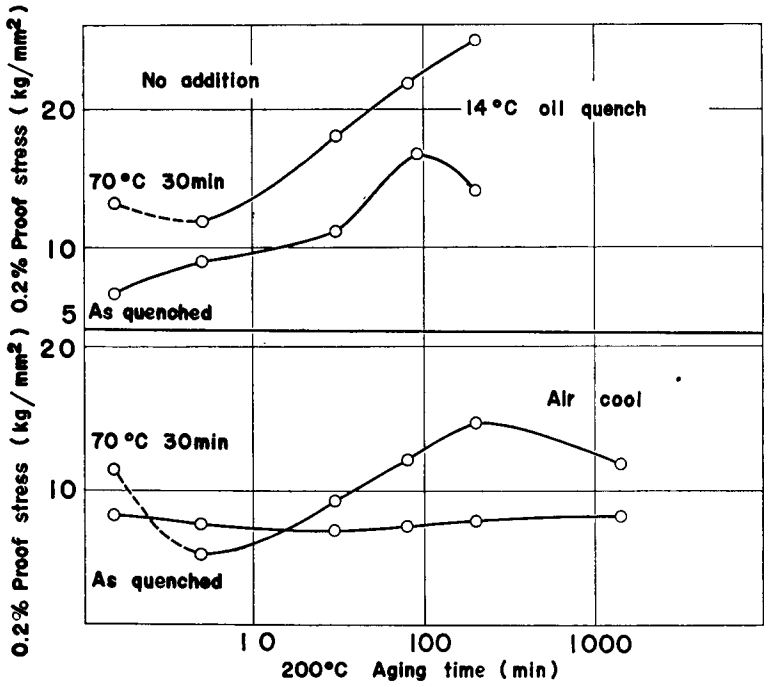

Fig. 29. Effect of the pre-aging of 30 min at 70°C on the age-hardening of the base alloy at 200°C.

Effect of trace addition of silver

Polmear[9] has reported the favorable effects of trace addition of Ag on this alloy system. In this experiment, from the point of a nucleation of η' intermediate phase, the effect of Ag was investigated. Fig. 30 shows the effect of quenching temperatures on the electrical resistivity of as-quenched specimens with or without Ag. There is very large difference between 400° and 500°C quenching

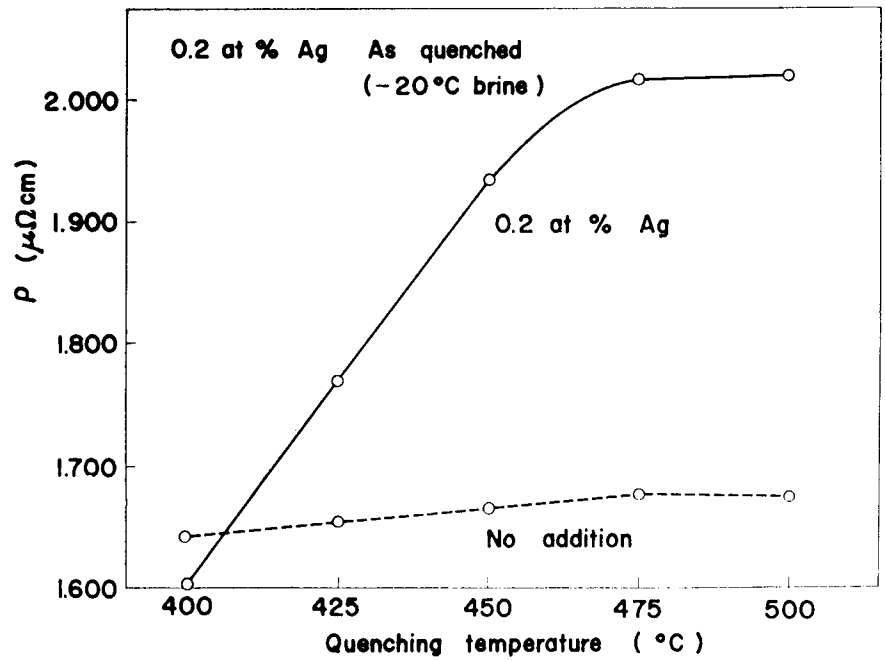

Fig. 30. Effect of the quenching temperature on the electrical resistivity of as-quenched specimens of the base alloy and the alloy added 0.2 at% Ag.

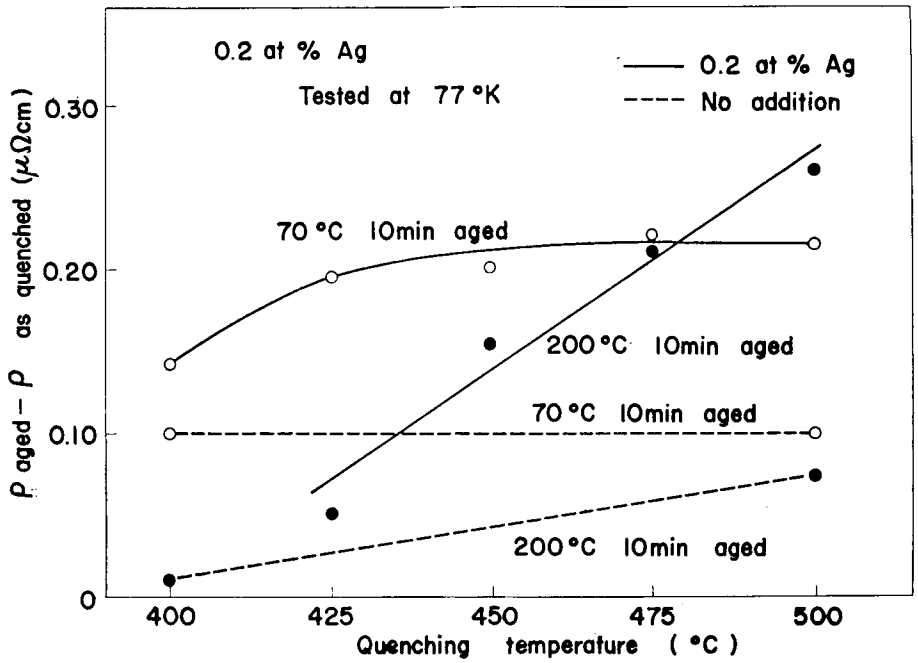

Fig. 31. Effect of the quenching temperature on the absolute value of electrical resistivity change of the base alloy and the alloy added 0.2 at% Ag, after several aging treatments.

for the specimen added 0.2% Ag. It seems to be one of the main reason that solute Ag atoms are dissolved into matrix when the solution temperature is raised, but it must be also taken into account that the clusters concerned with Ag are formed during or immediately after quenching. After a pre-annealing of 535°C for 1 hr, specimens were quenched into −20°C brine from several temperatures between 400°C and 535°C, and then aged at 70°C or 200°C. Fig. 31 and 32 show effects of quenching temperatures on electrical resistivity and strength respectively.

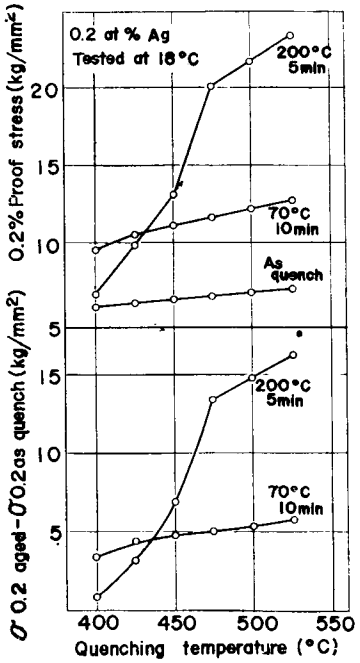

Fig. 32. Effect of the quenching temperature on 0.2% proof stress of the alloy added 0.2 at% Ag after some aging treatments (upper part) and the increase of 0.2% proof stress from that of as-quenched state (lower part).

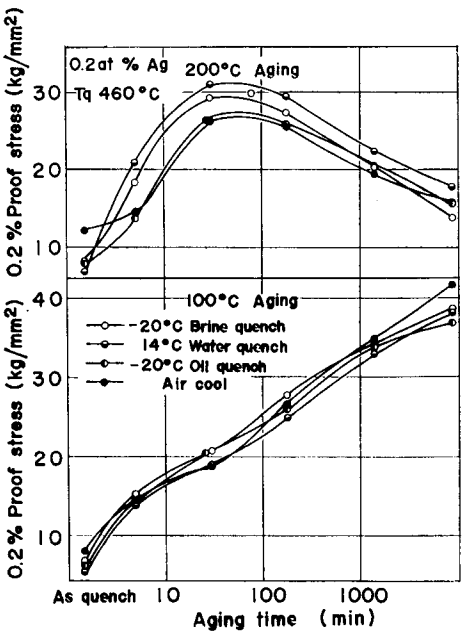

Fig. 33. Effect of the cooling rate on the age-hardening of the alloy added 0.2 at% Ag at 200°C (upper part) and 100°C (lower part).

Both properties for the specimens added Ag are shown to vary remarkably with quenching temperatures than of base alloys. Fig. 33 shows the effect of a change in quenching medium by the similar experimental procedure as in the case of Fig. 24. Changes of cooling rate influence little on the higher temperature aging of 200°C. This is quite different from that of base alloys as shown previously. It is concluded, therefore, that small additions of Ag have much favorable influence on the high temperature aging, where nucleation is very important for precipitation of η' intermediate phase. It is assumed that Ag accelerates the formation of

clusters during or immediately after quenching, which serves to assist the nucleation of η' intermediate phase when aged at higher temperature.

IV Conclusions

(1) The idealized solid solution of the alloys could not always be realized, and many imperfections such as sub-boundaries still remained, particularly when trace elements were added being dependent upon the temperature and time of a solution treatment. The imperfections will act as a vacancy sinks during quenching and, therefore, influence remarkably the following precipitation. The complete solid solution of this alloy is thought to be obtained at above about 500°C and, in the case of addition of Ag, Cu, or Cr, at much higher temperatures. Particularly, in the case of Cr, it needs to raise to about 550°C to obtain a complete solid solution.

(2) From the results of resistivity measurements, vacancy-solute clusters could be formed during or immediately after quenching. The size and number of clusters seem to depend upon the quenching methods. These clusters contribute considerably to the resistivity of the alloys, but only a little to strength of as-quenched specimens. When aged the quenched specimens, the resistivity increase caused by formation of G.P. zone is observed until temperature of 130°C is reached.

(3) Vacancy-solute clusters can act as precipitation nuclei of η' intermediate phase and, therefore, influence considerably on the high temperature aging. The effect of the quenching temperature and medium on the high temperature aging was shown to be explained from the size distribution of clusters.

(4) From the test temperature dependence of the strength in this alloy system, it might be true that precipitate produced by aging at low temperature or for short time at high temperature are cut through by moving dislocations.

(5) The favorable effects of a time interval or pre-aging between quenching and artificial aging on the hardening are found to exsist in this alloy for higher temperature aging.

(6) Small additions of Ag have much favorable influence on higher temperature aging. It is assumed that Ag accelerates the formation of clusters during or immediately after quenching, which serve to assist the nucleation of η' intermediate phase.

The present investigation was partially supported by a Research Fund provided by the Light Metal Educational Foundation, Inc. of Japan for which the authors wish to express their deep appreciation.

References

1) G. Kitahara and I. Igarashi: Nippon Kinzoku Gakkaishi **4** (1940) 343.
2) G. Kitahara and I. Igarashi: Nippon Kinzoku Gakkaishi **6** (1942) 313.
3) Y. Murakami: Keigokin yousetsu **22** (1964) 11.
4) T. Kobayashi: Buletin of Nippon Kinzoku Gakkai **3** (1964) 540.
5) W. Sander: Z. anorg. ally. chem. **154** (926).
6) M. Hamazumi: Tetsu to Hagane **22** (1936) 258.
7) W.L. Köster und W. Dullenkopf: Z. Metallk. **28** (1936) 363.
8) W.L. Fink and L.A. Willy: A.I.M.E. (1937) 78.
9) I.J. Polmear: J.I.M. **86** (1957–58) 113.
89 (1960–61) 51, 193.
90 (1961–62) 180.
94 (1966) 37.
10) L.F. Mondolfo, N A. Gjostein and D.W. Levinson: J. Metals **8** (1956) 1378.
11) R.B. Nicholson, G.J. Thomas and J. Nutting: J.I.M. **87** (1958–59) 429.
12) G.J. Thomas and J. Nutting: J.I.M. **88** (1959–60) 81.
13) J.D. Embury and R.B. Nicholson: J. Aust. I.M. **8** (1963) 76.
14 J.D. Embury and R.B. Nlcholson: Acta Met. **13** (1965) 403.
15) V.A. Phillips, A.J. Swain and R. Eborall: J.I.M. **81** (1992–53) 625, 659.
16) S. Terai and Y. Baba: Sumitomo Keikinzoku Giho **4** (1963) 173.
17) P.P. Kuzumenko: Ukrayinskii Fizychnyi Zhurnal **6** (1961) 116.
18) E. Orowan: Symposium on Internal Stress in Metals and Alloys (1948) Inst. of Metals.
19) P.B. Hirsh: J.I.M. **86** (1957) 13.
20) D. Turnbull, H.S. Rosenbaum and H.N. Treaftis: Acta Met. **8** (1960) 277.
21) W. Desorbo, H.N. Treaftis and D. Turnbull: Acta. Met **6** (1958) 401.
22) H. Kimura and R. Hashiguchi: Acta Met. **9** (1961) 1076.
23) M. Ohta and F. Hashimoto: J. Phys. Soc. Japan, **19** (1964) 130.
24) C. Panseri and T. Federighi: Acta Met. **8** (1960) 217.
25) N.F. Mott: J.I.M. **60** (1937) 267.
26) Z. Matyas: Phil. Mag. **7** (1949) 324.
27) A.H. Geisler: Phase Transformation in Solid, (1951) 387.
28) E.W. Hart: Acta Met. **6** (1958) 553.
29) T. Federighi and G. Thomas: Phil. Mag. **7** (1962) 127.
30) A. Kelly and R.B. Nicholson: Progress in Material Science, **10** (1963) 324.
31) A. Kelly and M.E. Fine: Acta Met. **5** (1957) 365.
32) N.F. Mott and F.R.N. Nabarro: Rep. Conf. Strength of Solid (1948).
33) A. Kelly: Phil. Mag. 8 **3** (1958) 1472.
34) R.O. Williams: Acta Met. **5** (1957) 385.
35) N.F. Motto: Phil. Mag. 8 **1** (1956) 568.
36) A. Seeger: Phil Mag. 4 **45** (1954) 771.
37) J. Dash and M.E. Fine: Acta Met. **9** (1961) 149.
38) J.G. Byrne, M.E. Fine and A. Kelly: Phil. Mag. 8 **6** (1961) 1119.
39) R.J. Price and A. Kelly: Acta Met. **12** (1964) 159.
40) R.L. Fleisher: Electron Microscopy and Strength of Crystals, (1963) Interscience, New York.
41) R.E. Smallman: Modern Physical Metallurgy, (1963) Batterworths, London, p. 293.
42) R.B. Nicholson: Electron Microscopy and Strength of Crystals, (1963) Interscience, New York, p. 861.
43) J.I. Taylor: J.I.M. **92** (1963–64) 301.
44) J.W. Cahn: Acta Met. **5** (1957) 169.
45) S. Nasu: private communication.
46) R. Horiuchi: Nippon Kinzoku Gakkaishi, **29** (1965) 85.

47) K. Shimizu: Rep. Light Metal Group, **1** (1965).
48) A.W. McReynolds: Trans A.I.M.E. **185** (1949) 32.
49) G.W. Ardley and A.H. Cottrel: Proc. Roy. Soc., A219 (1953) 328.
50) M.A. Adams, A.C. Roberts and R.E. Smallman: Acta Met. **8** (1960) 328.
51) J. Caisso: Mem. Sci. Rev. Met. **56** (1959) 237.
52) P.R. Sperry: Acta Met. **11** (1963) 153.
53) B.A. Riggs and L.J. Demer: Acta Met. **11** (1963) 1003.
54) Z. Basinski: Proc. Roy. Soc. A240 (1957) 229.
55) A.H. Cottrel: Phil. Mag. **44** (1953) 829.
56) E.C.W. Perryman: Acta Met. **3** (1955) 412.
57) B. Russel: Phil. Mag. **8** (1963) 615, 677.
58) B.A. Wilcox and G.C. Smith: Acta Met. **12** (1964) 371.
59) A.H. Cottrel: Rep. Conf. Strength of Solids, (1948) 30.
60) R.P. Agarwala, S.P. Murarka and M.S. Anand: Acta Met. **12** (1964) 871.
61) M. Ohta and F. Hashimoto: Nippon Kinzoku Gakkaishi **29** (1965) 272.
62) G. Bastsch: Acta Met. **12** (1964) 270.
63) C. Panseri and T. Federighi: Acta Met. **11** (1963) 575.
64) S. Koda and M. Nemoto: Nippon Kinzoku Gakkaishi, **29** (1965) 399, 406.
65) G.W. Lorimer and R.B. Nicholson: Acta Met. **14** (1966) 1009.
66) H.A. Hole: J. Inst. Metals **93** (1964–65) 364.
67) M.H. Jacobs, D.W. Pashley and J.T. Vietz: Sixth International Congress for Electron Microscopy, Kyoto (1966), 391.